

Two-dimensional ground motion at a soft viscoelastic layer/hard substratum site in response to SH cylindrical seismic waves radiated by deep and shallow line sources—I. Theory

Jean-Philippe Groby¹ and Armand Wirgin²

¹Laboratoire de Mécanique et d'Acoustique, UPR 7051 du CNRS, 31 chemin Joseph Aiguier, 13402 Marseille cedex 20, France

²LMA/CNRS, 31 chemin Joseph Aiguier, 13402 Marseille cedex 20, France. E-mail: wirgin@lma.cnrs-mrs.fr

Accepted 2005 June 14. Received 2005 February 9; in original form 2004 January 23

SUMMARY

We consider, using theory (herein) and associated synthetic seismograms (in a companion paper), the seismic response of a site comprising a horizontal, homogeneous, soft viscoelastic layer of infinite lateral extent overlying, and in welded contact with, a homogeneous, hard elastic substratum of half-infinite radial extent. We show that for shear-horizontal motion: (1) coupling to Love modes is all the stronger the closer (in the vertical direction) the source (modelled as a line, assumed to lie in the substratum) is to the lower boundary of the soft layer, (2) all anomalous features (such as long duration) of the seismic wavefield, including those for regional earthquakes, are primarily the result of strong excitation of Love modes, (3) 1-D (body wave) type of response is: non-resonant, obtained for deep sources and usually characterized by relatively short durations, (4) for shallow sources and hypocentral distances that are not very large, the response results from a complex interplay of Love mode and body wave contributions, which requires a numerical description (furnished in the companion paper).

Key words: duration, interference maxima, Love modes, regional path effects, site response, source position.

1 INTRODUCTION

This investigation is relevant to several topics of broad interest in seismic wave propagation:

(a) regional path effects in connection with seismic response in urban environments (Novikova & Trifunac 1993; Singh & Ordaz 1993; Faeh & Panza 1994; Faeh *et al.* 1994; Novikova & Trifunac 1995; Furumura & Kennett 1998; Hisada *et al.* 1988; Shapiro *et al.* 2000, 2001, 2002; Panza *et al.* 2001; Cárdenas & Chávez-García 2003; Celebi 2004; Savage 2004; Shoji *et al.* 2004; Balendra & Kong 2004),

(b) effects of the underlying soil heterogeneities, lateral variations of the underlying soil layer and built environment on seismic ground response at various (particularly urban) sites (Hisada *et al.* 1988; Faeh & Panza 1994; Faeh *et al.* 1994; Romanelli 1996; Chen *et al.* 1998; Furumura & Kennett 1998; Panza *et al.* 2000a,b; Semblat *et al.* 2000; Boore 2003; Semblat *et al.* 2003; Tsogka & Wirgin 2003; Celebi 2004; Sandi *et al.* 2004),

(c) analysis of surface wave response on the ground to determine the structure and composition of the crust (Ben-Zion & Aki 1990; Chen *et al.* 1998; Pollitz 1999; Snieder 2000; Savage 2004) and underground fault zones (Igel *et al.* 2002; Jahnke *et al.* 2002) and

(d) analysis of surface wave response on the ground to identify earthquake sources (Mendiguren 1977; Kanamori & Given 1981; Ben-Zion & Aki 1990).

Research on topic (a) was rekindled by efforts to explain some puzzling features of the devastating Michoacan earthquake which struck Mexico City in 1985 (Furumura & Kennett 1998). Other than the fact that the response in downtown Mexico varied considerably in a spatial sense, was quite intense and of very long duration (as much as ~3 min) (the notion of duration is examined in e.g. Trifunac & Brady 1975; Trifunac & Westermo 1976) at certain locations, and often took the form of a quasi-monochromatic signal with beating, a remarkable feature of this earthquake was that such strong (in the sense just mentioned) response could be caused by a seismic disturbance so far (its epicentre was in the subduction zone off the Pacific coast approximately 350 km) from the city (Chávez-García & Bard 1994; Faeh & Panza 1994; Faeh *et al.* 1994; Chávez-García *et al.* 1995; Furumura & Kennett 1998). A part of the cause of the large intensity and long duration was attributed in Singh & Ordaz (1993) to multipathing between the source and the site. This hypothesis was further explored in Chávez-García & Bard (1994) Chávez-García *et al.* (1995) and Furumura & Kennett (1998), while being associated with surface wave propagation of the Rayleigh and Love types, presumably between the source and the entry to the Mexico City basin, via the intervening crust.

In a rather complete (other than the neglect of attenuation) 3-D numerical study (Shapiro *et al.* 2000), the long duration and large amplitude of response at various distances from subduction zone earthquakes in Mexico were attributed to the entrapment of the seismic disturbance in an accretionary prism (wedge-shaped heterogeneity) of the crust and its subsequent propagation to the point of observation. The authors of this work later (Shapiro *et al.* 2001, 2002), as well as Furumura & Kennett (1998) somewhat earlier, stressed the role of higher-order surface waves, which propagate in the relatively high Q layer of the Trans Mexican Volcanic Belt (TMVB, composed of low-velocity volcanic lava and tuff overlying higher-velocity limestone) underlying the soft clay basin of Mexico City in producing large response (particularly with respect to duration) in the city. More recently, an analysis (Cárdenas & Chávez-García 2003) of seismograms recorded at various sites in central Mexico, for earthquake sources located in the subduction zone off the Pacific coast, has shown that the crustal structure (including that of the TMVB) between the source and observation points acts as a waveguide for surface waves coming from distances greater than 200 km, leading, by an unexplained mechanism, to amplification and increase of duration of motion at various sites, notably in Mexico City. Numerical results obtained in earlier studies (e.g. Faeh *et al.* 1994; Faeh & Panza 1994) with a rather complete, 2-D hybrid model of the propagation path between the source and the Mexico City basin, and of the action of the basin on the incident wave, also stressed the important role of regional path effects on anomalous response. The 3-D equivalent of these numerical simulations, carried out by Furumura & Kennett (1998), back up these findings.

Anomalous response in other cities such as Beijing, Bucharest, Rome, etc. has been studied in great detail, principally in a numerical manner, within the framework of the UNESCO-IGCP project 414 (Panza *et al.* 2000b, 2001). The features of this response were attributed (as in an earlier work by Campillo *et al.* 1989) to the specifics of the source parameters, regional path effects and the specifics of the soil distribution and geometry in the urban basins (see next paragraph). These findings have been substantiated in a more recent study (Boore 2003).

Topic (b) deals with a class of alternative or complementary (so-called local) paradigms for explaining seismic motion in urban sites built on soft soil. Even though the anomalous response in 1985 in Mexico City originated from a subduction zone source whose epicentral distance was some 350 km from the city, it has been common to seek explanations of this response [and others such as in Nice (Semblat *et al.* 2000, 2003) and Bucharest (Sandi *et al.* 2004)] by employing models involving vertically propagating or nearly vertically propagating plane waves. This requires that the focal depth (also known as the hypocentral depth (Novikova & Trifunac 1995)) be large and that the epicentral distance from the source to the city be rather small. Although both of these conditions are often not met in practice (and, in particular, as concerns the 1985 Michoacan earthquake), the vertically propagating plane wave solicitation usually prevails in the theoretical/numerical studies (Balendra & Kong 2004; Sandi *et al.* 2004; Semblat *et al.* 2004), apparently because it simplifies the analysis (another reason is that it facilitates comparison with the 1-D model of normally incident plane waves on a vertically layered half space). This has the effect of putting the focus on what occurs in the structure vertically below the city, namely, on the soft basin on which the earthquake-prone cities are built. Thus, a considerable number of studies (see Bard *et al.* 1988; Chávez-García & Bard 1994; Semblat *et al.* 2004, for comprehensive reviews) examine the (local) effect of the soft basin on the incident wave, but at present, it is thought that local effects account for only part of the anomalous response (Chávez-García & Bard 1994; Chávez-García *et al.* 1995; Panza *et al.* 2000b, 2001; Cárdenas & Chávez-García 2003; Boore 2003). On the other hand, Hisada *et al.* (1988) show that the position of the source relative to the basin is a critical factor for determining the ground response in the basin. Another idea that has been explored in the past few years is that the buildings of the city, in interaction with the soft soil and with each other, may also amplify and lengthen the duration of the ground motion (see Semblat *et al.* 2003; Tsogka & Wirgin 2003; Boutin & Roussillon 2004 for reviews of this subject). A majority of these studies (including or excluding the buildings) point to the central role of surface waves, qualified either as locally launched surface (e.g. Love) waves (at the basin edges or at heterogeneities of the soft soil) (Bard & Bouchon 1980; Bard *et al.* 1988; Faeh *et al.* 1994; Boore 2003) or as quasi-Love waves (excited at the base of the buildings and re-amplified by interaction with neighbouring buildings, Semblat *et al.* 2003; Tsogka & Wirgin 2003; Groby *et al.* 2004) as a possible causal agent of anomalous response, but little (Wirgin & Kouh-Bille 1993), if any, theoretical evidence has been given to back up these assertions.

Topic (c) is classical in seismological geophysics (Ewing *et al.* 1957). The seismic signals associated with various types of surface (e.g. Love and Rayleigh) waves are often-used tools for reconstructing features of the earth's crust such as thickness, composition (e.g. vertical layering characteristics (Ewing *et al.* 1957; Panza 1981; Snieder 2000) and even lateral heterogeneities (Wirgin 1988; Chen *et al.* 1998). More recently (Ben-Zion & Aki 1990; Igel *et al.* 2002; Jahnke *et al.* 2002), it has been shown that seismic sources in the neighborhood of fault zones (FZ, i.e. soft nearly vertical layers surrounded by relatively hard soil) excite surface waves (qualified as trapped) in the vicinity of the FZ, which propagate to the ground where they can be detected and used to furnish information on the physical and geometrical characteristics of the FZ. To treat these inverse problems in a fully unambiguous manner requires a thorough understanding of the way in which the seismic source interacts (notably how accurately one must know the position and characteristics of the source) with the inhomogeneities.

Topic (d) is also a classical one in seismology, the main concern being to localize and qualify (e.g. determine the moment tensor of) earthquake sources (Mendiguren 1977; Kanamori & Given 1981). As the seismic wave, including its surface-wave components, travels laterally (sometimes over long distances) in and along the crust before reaching the measurement locations on the ground, the inverse problem is difficult to solve if the crustal features (which can include lateral heterogeneity) are not known beforehand. In any case, it is important to determine the influence of errors of the crustal model on the reconstruction of the source location and moment tensor, and to do this requires an appropriate theoretical analysis.

The theoretical investigation herein (and the numerical study in the companion paper) is (are) focused on topics (a) and (b). In contrast to the *inverse-scattering* topics (c) and (d) (to which our analysis could be applied) wherein the response is known and the propagation medium and/or the source are to be determined, the problem we are faced with herein deals with *forward scattering*: given the seismic source and the characteristics of the propagation medium, determine the response (displacement in the frequency and/or time domain) on the ground. More specifically, we shall be concerned with a (deceivingly) simple canonical scattering problem: that of a cylindrical SH pulse wave impinging on a soft homogeneous layer, the latter being horizontal, of infinite lateral extent, bounded above by the free surface and below by an interface with a half-space filled with hard homogeneous rock. The questions we address, and that we think can be answered with the help of such a simple model, are:

- (i) is it possible to obtain anomalous (in the sense mentioned above in connection with the Michoacan earthquake) response without any lateral heterogeneity (arising from volumetric inclusions or unevenness of interfaces) in the underground medium?
- (ii) what is the relation of 1-D to 2-D response and how adequate is it to model the general response of the configuration by its response to a (nearly) vertically incident plane wave?
- (iii) how does the focal depth of the source affect the response?

In the companion paper (Groby & Wirgin 2005), we shall provide answers to the following questions (in addition to the previous ones, whenever numerics are judged to be necessary):

- (iv) how does the epicentral distance affect the response?
- (v) how does the contrast of mechanical properties between the layer and the half-space affect the ground response?
- (vi) how does the thickness of the layer affect the response?
- (vii) how do the spectral characteristics of the incident pulse affect the response?

It will be shown that a source radiating cylindrical waves in a fully elastic soft layer/hard half-space medium produces a ground response which is the sum of three terms corresponding to various combinations of two types of waves in the soft layer (SL) and hard half-space (HHS):

- (1) standing body waves (SBW) in the SL and body waves (BW) in the HHS,
- (2) standing body waves in the SL and surface waves (SW) in the HHS and
- (3) standing surface waves (SSW) in the SL and surface waves in the HHS.

Only type (2) waves correspond to Love modes (at the resonance frequencies of these modes) and the conditions for optimal excitation and maximal contribution of these modes will be rendered explicit. It will be shown theoretically that large-duration (i.e. anomalous) response generally requires a preponderant contribution of at least one (usually the lowest-order) of the Love modes to the overall response. The type (1) waves dominate in the situation in which the focal depth is large and do not usually produce *long-duration response*, although they can produce *strong (but normal) response* when the contrast of mechanical properties between the SL and HHS is large. Beating phenomena will be shown to be a consequence (for impulsive solicitations with predominantly low-frequency spectra) of interference between type (1) and type (2) waves which both lead to maxima in response at nearly the same (low) frequency. Type (3) waves turn out to have negligible contribution to overall response. Most of these features carry over to the case in which the layer is lossy. The practical consequences of these results, in relation to topics (a) and (b), will be discussed.

2 DESCRIPTION OF THE CONFIGURATION

Fig. 1 represents a cross-section (sagittal plane) view of a generic bare (i.e. all the constructions are eliminated) urban site. Γ_g is the ground, assumed to be flat and horizontal, above which is located the air medium, assumed to be the vacuum. Ω_1 is the laterally infinite domain occupied by the mechanically soft layer and h is its thickness. Ω_0 is the semi-infinite domain (substratum) occupied by a mechanically hard medium, and Γ_h the flat, horizontal interface between the layer and the substratum. A $Ox_1x_2x_3$ Cartesian coordinate system is attached to this configuration such that O is on the ground, x_2 increases with depth and x_3 is perpendicular to the (sagittal) plane of the figure. With \mathbf{i}_j the unit vector along the positive x_j axis, we note that the unit vectors normal to Γ_g and Γ_h are \mathbf{i}_2 . The media filling Ω_0 and Ω_1 are M^0 and M^1 , respectively and the latter are assumed to be initially stress free, linear, isotropic and homogeneous. We assume that M^0 is non-dissipative and M^1 is generally (unless specified otherwise) dissipative.

The seismic disturbance is delivered to the site in the form of a shear-horizontal (SH) cylindrical pulse wave radiated by a line source (perpendicular to the sagittal plane) located at $\mathbf{x}^s := (x_1^s, x_2^s)$, with, by hypothesis, $x_2^s > h$ (i.e. $\mathbf{x}^s \in \Omega_0$). The SH nature of this wave means that the motion associated with it is strictly transverse (i.e. in the x_3 direction and independent of the x_3 coordinate). Both the SH polarization and the invariance of the incident wave with respect to x_3 are communicated to the fields that are generated at the site in response to the incident wave. Thus, our analysis will deal only with the propagation of 2-D SH waves (i.e. waves that depend exclusively on the two Cartesian coordinates x_1, x_2 and that are associated with motion in the x_3 direction only).

We shall be concerned with a description of the elastodynamic wavefield on the ground (i.e. on Γ_g) resulting from the cylindrical seismic wave solicitation of the site.

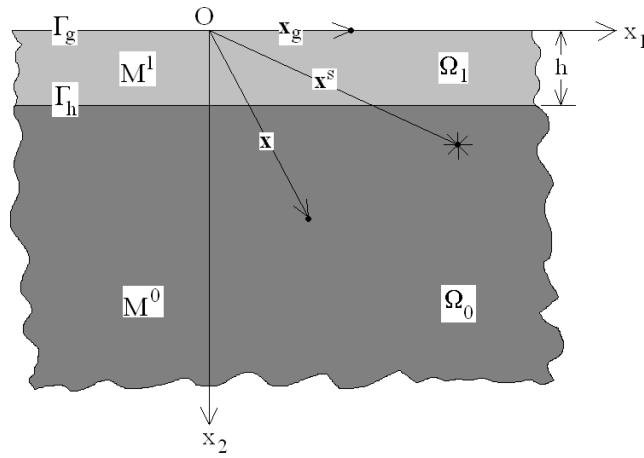


Figure 1. Cross-section view of the configuration.

3 GOVERNING EQUATIONS

3.1 Space–time domain wave equations

In a generally inhomogeneous, isotropic elastic or viscoelastic medium M occupying \mathbb{R}^3 , the time-domain wave equation for SH waves is:

$$\nabla \cdot (\mu(\mathbf{x}, \omega) \nabla u(\mathbf{x}, t)) - \rho(\mathbf{x}) \partial_t^2 u(\mathbf{x}, t) = -\rho(\mathbf{x}) f(\mathbf{x}, t), \tag{1}$$

wherein u is the displacement component in the \mathbf{i}_3 direction, f the component of applied force density in the \mathbf{i}_3 direction, μ the Lamé descriptor of rigidity, ρ the mass density, t the time variable, ω the angular frequency, ∂_t^n the n th partial derivative with respect to t , and $\mathbf{x} = (x_1, x_2)$. Since our configuration involves two homogeneous media and the applied force is assumed to be non-vanishing only in Ω_0 , we have

$$(c^m(\omega))^2 \nabla \cdot \nabla u^m(\mathbf{x}, t) - \partial_t^2 u^m(\mathbf{x}, t) = -f(\mathbf{x}, t) \delta_{m0}; \mathbf{x} \in \Omega_m, \tag{2}$$

wherein m superscripts designate the medium (0 for M^0 or 1 for M^1), $\delta_{m0} = 1$ for $m = 0$ and equal to zero otherwise, and c^m is the generally complex velocity of shear body waves in M^m , related to the density and rigidity by

$$(c^m(\omega))^2 = \frac{\mu^m(\omega)}{\rho^m}, \tag{3}$$

it being understood that $\rho^m, \mu^m(\omega); m = 0, 1$ are constants with respect to \mathbf{x} .

3.2 Space–time domain representation of the force

In all that follows we choose a line source force function

$$f(\mathbf{x}, t) = -\delta(\mathbf{x} - \mathbf{x}^s) S(t), \tag{4}$$

wherein $\delta(\cdot)$ is the Dirac delta distribution and \mathbf{x}^s designates the position of the line source.

3.3 Space–frequency domain wave equations

The frequency-domain versions of the wave equations are obtained by expanding the force density and displacement in Fourier integrals:

$$f(\mathbf{x}, t) = \int_{-\infty}^{\infty} f(\mathbf{x}, \omega) e^{-i\omega t} d\omega, \quad u^m(\mathbf{x}, t) = \int_{-\infty}^{\infty} u^m(\mathbf{x}, \omega) e^{-i\omega t} d\omega, \quad \forall t \in \mathbb{R}, \tag{5}$$

so as to give rise to the Helmholtz equations

$$\nabla \cdot \nabla u^m(\mathbf{x}, \omega) + (k^m(\omega))^2 u^m(\mathbf{x}, \omega) = -f(\mathbf{x}, \omega) \delta_{m0}; \quad \forall \mathbf{x} \in \Omega_m; \quad m = 0, 1, \tag{6}$$

wherein

$$k^m(\omega) := \frac{\omega}{c^m(\omega)} = \omega \sqrt{\frac{\rho^m}{\mu^m(\omega)}} \tag{7}$$

is the generally complex wavenumber in M^m . Actually, due to the assumptions made in Section 2:

$$k^0(\omega) := \frac{\omega}{c^0} = \omega \sqrt{\frac{\rho^0}{\mu^0}}, \tag{8}$$

(i.e. k^0 is real),

$$f^m(\mathbf{x}, \omega) = S(\omega)\delta(\mathbf{x} - \mathbf{x}^s), \quad (9)$$

wherein $S(\omega)$ is the spectrum of the incident pulse.

3.4 Material constants in the dissipative medium

A word is now in order about the dissipative nature of the layer. When a medium M is lossy, the wavenumber therein is complex and can be written (omitting, for the moment, the ω dependence) as

$$k = k' + ik'', \quad (10)$$

where, by convention,

$$\Re k = k' \geq 0, \quad \Im k = k'' \geq 0. \quad (11)$$

We now refer to (7) and note that complex k implies complex μ , due to the fact that it is advisable to consider the mass density to be a real quantity. Thus, we write

$$\mu = \mu' - i\mu''. \quad (12)$$

In order to retain the positive real aspect of the rigidity for elastic materials, we take

$$\Re \mu = \mu' \geq 0, \quad (13)$$

and inquire as to the sign of the imaginary part of μ . Introducing (12) into (7) gives

$$k = \omega\rho^{1/2}(\mu' - i\mu'')^{-1/2} = \omega \left(\frac{\mu'}{\rho} \right)^{-1/2} \left[1 - i \frac{\mu''}{\mu'} \right]^{-1/2}. \quad (14)$$

We assume, as is generally the case for moderately dissipative media, that $|\mu''/\mu'| \ll 1$, so that a Taylor series expansion of $[]^{-1/2}$ limited to the first two terms yields

$$k = k' + ik'' \approx \frac{\omega}{c'} \left[1 + i \frac{\mu''}{2\mu'} \right], \quad (15)$$

wherein, by definition,

$$c' = \left(\frac{\mu'}{\rho} \right)^{1/2}. \quad (16)$$

Making use of (11) and (12) thus necessarily leads to

$$\Im \mu = -\mu'' \leq 0. \quad (17)$$

We define the positive real quantity known as the quality factor Q by the ratio

$$Q := \frac{\mu'}{\mu''}, \quad (18)$$

and note that it is infinite for a lossless medium such as M^0 (because $\mu'' = 0$ in this case). Furthermore, the complex wavenumber becomes

$$k = k' + ik'' = \frac{\omega}{c'} \left(1 + \frac{i}{2Q} \right), \quad (19)$$

from which we find

$$Q = \frac{k'}{2k''}. \quad (20)$$

A question arises as to the proper definition of the complex body wave velocity c in M . We write

$$c = c' - ic'', \quad (21)$$

and require

$$\Re c = c' \geq 0, \quad (22)$$

due to the fact that the body wave velocity is positive in a non-lossy medium. We have

$$k = k' + ik'' = \frac{\omega}{c} = \frac{\omega}{c' - ic''} = \frac{\omega c' + i\omega c''}{|c|^2}, \quad (23)$$

from which we see that in order for $\Im k = k'' \geq 0$, we must have

$$\Im c = -c'' \leq 0. \quad (24)$$

The remaining question is that of the ω -dependence of μ and Q (the ω -dependence of k and c follows from that of μ and Q). In seismological applications involving viscoelastic media the quality factor is found to be either constant or a weakly varying function of frequency (Faeh

et al. 1994). We shall assume that $Q^1(\omega) = Q^1 = \text{const.}$, and it can be shown (Kjartansson 1979) that this implies

$$\mu^1(\omega) = \mu_{\text{ref}}^1 \left(\frac{-i\omega}{\omega_{\text{ref}}} \right)^{\frac{2}{\pi} \arctan\left(\frac{1}{Q^1}\right)}, \quad (25)$$

wherein: ω_{ref} is a reference angular frequency, preferably as close as possible to zero, but chosen herein, for numerical reasons, to be equal to 9×10^{-2} Hz. Hence

$$c^1(\omega) = c_{\text{ref}}^1 \left(\frac{-i\omega}{\omega_{\text{ref}}} \right)^{\frac{1}{\pi} \arctan\left(\frac{1}{Q^1}\right)}, \quad (26)$$

and

$$c_{\text{ref}}^1 := \sqrt{\frac{\mu_{\text{ref}}^1}{\rho^1}}. \quad (27)$$

Note should be taken of the fact that even though Q^1 is non-dispersive (i.e. does not depend on ω) under the present assumption, the phase velocity c^1 is dispersive.

3.5 Boundary and radiation conditions

We assume the layer and the substratum to be in *welded contact* so that the displacement and the tangential components of traction are continuous across the interface Γ_h :

$$u^1(\mathbf{x}, \omega) - u^0(\mathbf{x}, \omega); \quad \mathbf{x} \in \Gamma_h, \quad (28)$$

$$\mu^1(\omega) \partial_n u^1(\mathbf{x}, \omega) - \mu^0(\omega) \partial_n u^0(\mathbf{x}, \omega); \quad \mathbf{x} \in \Gamma_h. \quad (29)$$

Since the air/layer interface Γ_g (i.e. the ground) is assumed to separate the vacuum from an elastic medium, the tangential component of traction must vanish on this boundary, that is,

$$\mu^1(\omega) \partial_n u^1(\mathbf{x}, \omega) = 0; \quad \mathbf{x} \in \Gamma_g, \quad (30)$$

wherein $\partial_n = \mathbf{i}_2 \cdot \nabla = \partial_{x_2}$. The uniqueness of the solution to the forward-scattering problem is assured by the radiation condition in the substratum:

$$u^0(\mathbf{x}, \omega) \sim \text{outgoing waves, } \|\mathbf{x}\| \rightarrow \infty, \quad x_2 > h. \quad (31)$$

3.6 Statement of the boundary-value (forward-scattering) problem

The problem is to determine the time record of the ground displacement field $u^1(\mathbf{x}_g, t)$ (with $\mathbf{x}_g := (x_1, 0)$) from the spectrum of the ground displacement $u^1(\mathbf{x}_g, \omega)$ via the Fourier transform

$$u^1(\mathbf{x}_g, t) = \int_{-\infty}^{\infty} u^1(\mathbf{x}_g, \omega) e^{-i\omega t} d\omega. \quad (32)$$

Note that due to the fact that $u^1(\mathbf{x}_g, t)$ is a real function, we must have

$$[u^1(\mathbf{x}_g, \omega)]^* = u^1(\mathbf{x}_g, -\omega), \quad (33)$$

(wherein the symbol $*$ designates the complex conjugate operator) from which it follows that

$$u^1(\mathbf{x}_g, t) = 2\Re \int_0^{\infty} u^1(\mathbf{x}_g, \omega) e^{-i\omega t} d\omega. \quad (34)$$

4 EXACT SOLUTIONS IN THE FREQUENCY DOMAIN BY SEPARATION OF VARIABLES

4.1 Preliminaries

Although the material in this section is classical as regards the way that plane wave integral representations of the fields are obtained, the manner in which these integrals are decomposed and analysed is somewhat different from previous investigations (e.g. Attwood 1951; Collins 1960; Harkrider 1964; Ben-Menahem & Harkrider 1964, 1970; Tuan & Ponomgi 1972; Bouchon 1982; Apsel & Luco 1983; Luco & Apsel 1983; Kennett 1983; Panza 1985; Van der Hijden 1987; Dravinski & Mossessian 1988; Ling *et al.* 1998; Zhang *et al.* 2003). The considerable quantity and variety of these publications attests to the richness and importance of the subject (which concerns electromagnetic, ultrasonic as

well as seismic waves), and to the fact that certain features of the subject are still obscure. In a first subclass of these investigations (to which we devote a discussion in an appendix of the companion paper Groby & Wirgin 2005), the plane wave integrals (with the horizontal wavenumber as the variable of integration) are reduced to residue series (so-called modal series) plus branch cut integrals, the latter being usually neglected if the source-to-observation point is large compared to the wavelength. In a second subclass of the aforementioned investigations, various devices are employed to evaluate, in numerically efficient, accurate, or asymptotic manners, the plane wave integrals. A third approach, associated with the so-called Cagniard -De Hoop method (Van der Hijden 1987), involves obtaining the time history without first determining the response spectrum in explicit manner.

Our contribution is essentially twofold: (1) establish the physical significance of the terms entering into our choices of the decomposition of the integrals, and (2) verify by numerical means, whenever possible, the theoretical predictions and discover new features of the ground response not immediately apparent in the theoretical formulae. The first task is undertaken in the present work, whereas the second task is accomplished in the companion paper (Groby & Wirgin 2005).

4.2 Frequency-domain solutions in the absence of the layer and the free surface

In the absence of the layer and the free surface, the problem is that of the radiation of a *SH* wave from a line source in 2-D free space (\mathbb{R}^2) occupied by the homogeneous medium M^0 . We term this radiated wave the ‘incident wave’ and designate it by u^i .

By applying separation of variables in the Cartesian coordinate system to the Helmholtz equation and using the radiation condition, it can be shown that u^i takes the form (Morse & Feshbach 1953)

$$u^i(\mathbf{x}, \omega) = \frac{i}{4\pi} S(\omega) \int_{-\infty}^{\infty} e^{i[k_1(x_1-x_1^s)+k_2^0(\omega)|x_2-x_2^s|]} \frac{dk_1}{k_2^0}, \quad (35)$$

or

$$u^i(\mathbf{x}, \omega) = \frac{i}{4} S(\omega) H_0^{(1)}(k^0(\omega) \|\mathbf{x} - \mathbf{x}^s\|), \quad (36)$$

wherein $H_0^{(1)}(\cdot)$ is the zeroth-order Hankel function of the first kind and:

$$k_2^j(\omega) := \sqrt{(k^j(\omega))^2 - k_1^2}, \quad \Re k_2^j(\omega) \geq 0, \quad \Im k_2^j(\omega) \geq 0, \quad j = 0, 1, \quad (37)$$

for real k_1 . We shall make use in Section 4.4 of the form taken by u^i in the region $\Omega_0^- := \{x_2^s > x_2 > h; \quad \forall x_1 \in \mathbb{R}\}$:

$$u^i(\mathbf{x}, \omega) = \int_{-\infty}^{\infty} A^0(k_1, \omega) e^{i[k_1 x_1 - k_2^0(\omega) x_2]} dk_1; \quad \forall \mathbf{x} \in \Omega_0^-, \quad (38)$$

wherein

$$A^0(k_1, \omega) = S(\omega) \frac{i}{4\pi k_2^0(\omega)} e^{-i[k_1 x_1^s - k_2^0(\omega) x_2^s]}. \quad (39)$$

4.3 Field representations in Cartesian coordinates for the configuration including the layer and the free surface

When the layer and free surface are present, the incident field described in the previous section cannot proceed in an unobstructed manner, that is, it gives rise to a ‘diffracted’ field (indicated by the superscript ‘*d*’) so that by re-use of separation of variables in Cartesian coordinates and the radiation condition we are led to represent the total fields in the substrate and the layer by

$$u^0(\mathbf{x}, \omega) = u^i(\mathbf{x}, \omega) + u^{0d}(\mathbf{x}, \omega), \quad (40)$$

$$u^1(\mathbf{x}, \omega) = u^{1d}(\mathbf{x}, \omega), \quad (41)$$

wherein:

$$u^{0d}(\mathbf{x}, \omega) = \int_{-\infty}^{\infty} B^0(k_1, \omega) e^{i[k_1 x_1 + k_2^0(\omega)(x_2 - h)]} dk_1; \quad x_2 > h, \quad \forall x_1 \in \mathbb{R}, \quad (42)$$

$$u^{1d}(\mathbf{x}, \omega) = \int_{-\infty}^{\infty} (A^1(k_1, \omega) e^{i[k_1 x_1 - k_2^1(\omega) x_2]} + B^1(k_1, \omega) e^{i[k_1 x_1 + k_2^1(\omega) x_2]}) dk_1; \quad 0 < x_2 < h, \quad \forall x_1 \in \mathbb{R}, \quad (43)$$

it being understood that the diffraction coefficients B^0 , A^1 , B^1 are, as yet, undetermined.

4.4 Determination of the diffraction coefficients and frequency-domain fields by application of the boundary conditions

The free-surface boundary condition entails:

$$A^1(k_1, \omega) = B^1(k_1, \omega), \quad \forall k_1 \in \mathbb{R}, \quad (44)$$

whence

$$u^{1d}(\mathbf{x}, \omega) = 2 \int_{-\infty}^{\infty} A^1(k_1, \omega) e^{ik_1 x_1} \cos(k_2^1(\omega) x_2) dk_1; \quad 0 < x_2 < h, \quad \forall x_1 \in \mathbb{R}. \quad (45)$$

The continuity of displacement condition leads to:

$$B^0(k_1, \omega) - 2A^1(k_1, \omega) \cos(k_2^1(\omega)h) = -A^0(k_1, \omega) e^{-ik_2^0(\omega)h}; \quad \forall k_1 \in \mathbb{R}, \quad (46)$$

whereas the continuity of tangential traction boundary condition implies:

$$i\mu^0(\omega)k_2^0(\omega)B^0(k_1, \omega) + 2\mu^1 k_2^1(\omega)A^1(k_1, \omega) \sin(k_2^1(\omega)h) = i\mu^0(\omega)k_2^0(\omega)A^0(k_1, \omega) e^{-ik_2^0(\omega)h}; \quad \forall k_1 \in \mathbb{R}. \quad (47)$$

The solution of this linear system of equations is:

$$B^0(k_1, \omega) = A^0(k_1, \omega) e^{-ik_2^0(\omega)h} \times \left(\frac{-\mu^1(\omega)k_2^1(\omega) \sin(k_2^1(\omega)h) + i\mu^0(\omega)k_2^0(\omega) \cos(k_2^1(\omega)h)}{\mu^1(\omega)k_2^1(\omega) \sin(k_2^1(\omega)h) + i\mu^0(\omega)k_2^0(\omega) \cos(k_2^1(\omega)h)} \right); \quad \forall k_1 \in \mathbb{R}, \quad (48)$$

$$A^1(k_1, \omega) = \frac{A^0(k_1, \omega)}{2} e^{-ik_2^0(\omega)h} \times \left(\frac{2i\mu^0(\omega)k_2^0(\omega)}{\mu^1(\omega)k_2^1(\omega) \sin(k_2^1(\omega)h) + i\mu^0(\omega)k_2^0(\omega) \cos(k_2^1(\omega)h)} \right); \quad \forall k_1 \in \mathbb{R}, \quad (49)$$

so that the solutions for the fields in the frequency domain are:

$$u^0(\mathbf{x}, \omega) = S(\omega) \int_{-\infty}^{\infty} \frac{i}{4\pi k_2^0(\omega)} e^{i[k_1(x_1 - x_1^s) + k_2^0(\omega)(x_2 - x_2^s)]} dk_1 \\ + S(\omega) \int_{-\infty}^{\infty} \frac{i}{4\pi k_2^0(\omega)} \left[\frac{i\mu^0(\omega)k_2^0(\omega) \cos(k_2^1(\omega)h) - \mu^1(\omega)k_2^1(\omega) \sin(k_2^1(\omega)h)}{i\mu^0(\omega)k_2^0(\omega) \cos(k_2^1(\omega)h) + \mu^1(\omega)k_2^1(\omega) \sin(k_2^1(\omega)h)} \right] \\ \times e^{i[k_1(x_1 - x_1^s) + k_2^0(\omega)(x_2 + x_2^s - 2h)]} dk_1; \quad \forall \mathbf{x} \in \Omega_0, \quad (50)$$

$$u^1(\mathbf{x}, \omega) = u^{1d}(\mathbf{x}, \omega) \\ = S(\omega) \int_{-\infty}^{\infty} \frac{i}{4\pi k_2^0(\omega)} \left[\frac{2i\mu^0(\omega)k_2^0(\omega)}{i\mu^0(\omega)k_2^0(\omega) \cos(k_2^1(\omega)h) + \mu^1(\omega)k_2^1(\omega) \sin(k_2^1(\omega)h)} \right] \\ \times \cos(k_2^1(\omega)x_2) e^{i[k_1(x_1 - x_1^s) - k_2^0(\omega)(h - x_2^s)]} dk_1; \quad \forall \mathbf{x} \in \Omega_1. \quad (51)$$

Finally, the frequency-domain ground response takes the form:

$$u^1(\mathbf{x}_g, \omega) = S(\omega) \int_{-\infty}^{\infty} \frac{i}{4\pi k_2^0(\omega)} \left[\frac{2i\mu^0(\omega)k_2^0(\omega)}{i\mu^0(\omega)k_2^0(\omega) \cos(k_2^1(\omega)h) + \mu^1(\omega)k_2^1(\omega) \sin(k_2^1(\omega)h)} \right] \\ \times e^{i[k_1(x_1 - x_1^s) - k_2^0(\omega)(h - x_2^s)]} dk_1; \quad \forall \mathbf{x} \in \Omega_1. \quad (52)$$

5 STRUCTURE OF THE FREQUENCY-DOMAIN RESPONSE IN THE CASE OF A NON-LOSSY LAYER

5.1 Frequency-domain response in the layer

When the layer is free of dissipation, that is, elastic, then μ^1 is real and does not depend on ω , and $k^1(\omega)$ is real (recall that we assumed the substratum to be elastic, which means that μ^0 is real and does not depend on ω , and $k^0(\omega)$ is real also). Consequently, in the integrals of the previous section we encounter intervals of k_1 over which k_2^0 and k_2^1 are either purely real or purely imaginary:

$$k_2^j(\omega) = K_2^j(\omega) := \left\| \sqrt{(k^j(\omega))^2 - k_1^2} \right\|; \quad |k_1| \leq k^j(\omega); \quad \omega \geq 0, \quad (53)$$

$$k_2^j(\omega) = i\kappa_2^j(\omega) := i \left\| \sqrt{k_1^2 - (k^j(\omega))^2} \right\|; \quad |k_1| \geq k^j(\omega); \quad \omega \geq 0. \quad (54)$$

It is important to note that the terms ‘soft layer’ and (relatively) ‘hard substratum’ have the following meaning in the present context:

$$c^0(\omega) > c^1(\omega) \Rightarrow k^0(\omega) < k^1(\omega), \quad (55)$$

$$\mu^0 > \mu^1, \quad (56)$$

so that (51) can be expressed as:

$$u^1(\mathbf{x}, \omega) = I_1^1(\mathbf{x}, \omega) + I_2^1(\mathbf{x}, \omega) + I_3^1(\mathbf{x}, \omega); \quad \forall \mathbf{x} \in \Omega_1, \quad (57)$$

with:

$$I_1^1(\mathbf{x}, \omega) = \int_{-k^0}^{k^0} du_1^1(\mathbf{x}, \mathbf{x}_g, k_1, \omega) = -\frac{S(\omega)}{2\pi} \int_{-k^0}^{k^0} F_1^1(k_1, \omega) \cos(K_2^1(\omega)x_2) e^{i[k_1(x_1-x_1^s) - K_2^0(\omega)(h-x_2^s)]} dk_1, \quad (58)$$

$$F_1^1(k_1, \omega) = \frac{\mu^0}{i\mu^0 K_2^0(\omega) \cos(K_2^1(\omega)h) + \mu^1 K_2^1(\omega) \sin(K_2^1(\omega)h)}, \quad (59)$$

$$\begin{aligned} I_2^1(\mathbf{x}, \omega) &= \left[\int_{-k^1}^{-k^0} + \int_{k^0}^{k^1} \right] du_2^1(\mathbf{x}, \mathbf{x}_g, k_1, \omega) = \\ &= -\frac{S(\omega)}{2\pi} \left[\int_{-k^1}^{-k^0} + \int_{k^0}^{k^1} \right] F_2^1(k_1, \omega) \cos(K_2^1(\omega)x_2) \\ &\quad \times e^{i[k_1(x_1-x_1^s) + \kappa_2^0(\omega)(h-x_2^s)]} dk_1, \end{aligned} \quad (60)$$

$$F_2^1(k_1, \omega) = \frac{\mu^0}{-\mu^0 \kappa_2^0(\omega) \cos(K_2^1(\omega)h) + \mu^1 K_2^1(\omega) \sin(K_2^1(\omega)h)}, \quad (61)$$

$$\begin{aligned} I_3^1(\mathbf{x}, \omega) &= \left[\int_{-\infty}^{-k^1} + \int_{k^1}^{\infty} \right] du_3^1(\mathbf{x}, \mathbf{x}_g, k_1, \omega) = \\ &= -\frac{S(\omega)}{2\pi} \left[\int_{-\infty}^{-k^1} + \int_{k^1}^{\infty} \right] F_3^1(\mathbf{x}_g, k_1, \omega) \cosh(\kappa_2^1(\omega)x_2) \\ &\quad \times e^{i[k_1(x_1-x_1^s) + \kappa_2^0(\omega)(h-x_2^s)]} dk_1, \end{aligned} \quad (62)$$

$$F_3^1(k_1, \omega) = \frac{-\mu^0}{\mu^0 \kappa_2^0(\omega) \cosh(\kappa_2^1(\omega)h) + \mu^1 \kappa_2^1(\omega) \sinh(\kappa_2^1(\omega)h)}. \quad (63)$$

We write:

$$du_1^1(\mathbf{x}, \mathbf{x}_g, k_1, \omega) = (G_1^1(\mathbf{x}_g, k_1, \omega) e^{i[k_1 x_1 + K_2^1(\omega)x_2]} + G_1^1(\mathbf{x}_g, k_1, \omega) e^{i[k_1 x_1 - K_2^1(\omega)x_2]}) dk_1, \quad (64)$$

$$G_1^1(\mathbf{x}_g, k_1, \omega) = -\frac{S(\omega)}{\pi} F_1^1(k_1, \omega) e^{-i[k_1 x_1^s + K_2^0(\omega)(h-x_2^s)]}, \quad (65)$$

which, together with (58), express the fact that a part (i.e. I_1^1) of the field in the layer is composed of a sum of standing body waves (SBW), each of which is the sum of two plane body waves having wavevectors with the same length.

In the same manner, we write:

$$du_2^1(\mathbf{x}, \mathbf{x}_g, k_1, \omega) = (G_2^1(\mathbf{x}_g, k_1, \omega) e^{i[k_1 x_1 + K_2^1(\omega)x_2]} + G_2^1(\mathbf{x}_g, k_1, \omega) e^{i[k_1 x_1 - K_2^1(\omega)x_2]}) dk_1, \quad (66)$$

$$G_2^1(\mathbf{x}_g, k_1, \omega) = -\frac{S(\omega)}{\pi} F_2^1(k_1, \omega) e^{-i[k_1 x_1^s + \kappa_2^0(\omega)(h-x_2^s)]}, \quad (67)$$

which, together with (60), express the fact that another part (i.e. I_2^1) of the field in the layer is again composed of a sum of standing body waves, each of which is the sum of two plane body waves with wavevectors having the same length. Note however that neither the wavevectors nor the amplitudes of these SBW are the same as those of the SBW (henceforth termed SBW1) in I_1^1 (because the range of integration in the latter is different from that in I_2^1). In fact, (67) tells us that the amplitudes G_2^1 of the SBW in I_2^1 (henceforth termed SBW2) decrease exponentially as the focal depth (i.e. x_2^s) increases, so that *the SBW2 make themselves felt all the less the farther the source is (in the vertical direction) from the ground*. On the other hand, the amplitudes of the SBW1 are sinusoidal functions of focal depth, so that *the SBW1 can possibly make themselves felt strongly for a large variety of source locations*.

Finally, we write:

$$du_3^1(\mathbf{x}, \mathbf{x}_g, k_1, \omega) = (G_3^1(\mathbf{x}_g, k_1, \omega) e^{i[k_1 x_1 + \kappa_2^1(\omega)x_2]} + G_3^1(\mathbf{x}_g, k_1, \omega) e^{i[k_1 x_1 - \kappa_2^1(\omega)x_2]}) dk_1, \quad (68)$$

$$G_3^1(\mathbf{x}_g, k_1, \omega) = -\frac{S(\omega)}{\pi} F_3^1(k_1, \omega) e^{-i[k_1 x_1^s + \kappa_2^0(\omega)(h-x_2^s)]}, \quad (69)$$

which, together with (62), express the fact that the third part (i.e. I_3^1) of the field in the layer is composed of a sum of standing surface waves (SSW), each of which is the sum of two plane surface waves with wavevectors having the same length (note that each such plane surface

wave is an inhomogeneous wave (with complex wavevector) whose phase is constant on $x_1 = \text{const.}$ and whose amplitude either increases or decreases as x_2 approaches some horizontal surface $x_2 = \text{const.}$) Eq. (69) tells us that the amplitudes G_3^1 of the SSW in I_3^1 decrease exponentially as the focal depth increases, so that *the SSW make themselves felt all the less the farther the source is (in the vertical direction) from the ground.*

The main conclusion of this discussion is that for focal depths of the source that are sufficiently large, the frequency-domain response in the layer is essentially given by I_1^1 and is expressed by a sum of SBW1. This corresponds more or less to the situation in the quasi-1-D analysis of the forward-scattering problem, but, as we shall see further on, it is, by no means, a valid picture of the response of the configuration when the focal depth of the source is not large.

5.2 Frequency-domain response in the hard half-space

We shall concentrate our attention exclusively on the diffracted field in the subdomain Ω_0^- although the essence of what will be written applies to the whole half-space Ω_0 . Proceeding as in Section 5.1 we find:

$$u^{0d}(\mathbf{x}, \omega) = I_1^0(\mathbf{x}, \omega) + I_2^0(\mathbf{x}, \omega) + I_3^0(\mathbf{x}, \omega); \quad \forall \mathbf{x} \in \Omega_0, \quad (70)$$

with:

$$\begin{aligned} I_1^0(\mathbf{x}, \omega) &= \int_{-k^0}^{k^0} du_1^0(\mathbf{x}, \mathbf{x}_g, k_1, \omega) \\ &= \frac{S(\omega)}{4\pi} \int_{-k^0}^{k^0} F_1^0(k_1, \omega) e^{i[k_1(x_1 - x_1^s) + K_2^0(\omega)(x_2 + x_2^s - 2h)]} dk_1, \end{aligned} \quad (71)$$

$$F_1^0(k_1, \omega) = \frac{i}{K_2^0(\omega)} \frac{i\mu^0 K_2^0(\omega) \cos(K_2^1(\omega)h) - \mu^1 K_2^1(\omega) \sin(K_2^1(\omega)h)}{i\mu^0 K_2^0(\omega) \cos(K_2^1(\omega)h) + \mu^1 K_2^1(\omega) \sin(K_2^1(\omega)h)}, \quad (72)$$

$$\begin{aligned} I_2^0(\mathbf{x}, \omega) &= \left[\int_{-k^1}^{-k^0} + \int_{k^0}^{k^1} \right] du_2^0(\mathbf{x}, \mathbf{x}_g, k_1, \omega) \\ &= \frac{S(\omega)}{4\pi} \left[\int_{-k^1}^{-k^0} + \int_{k^0}^{k^1} \right] F_2^0(k_1, \omega) e^{i[k_1(x_1 - x_1^s) - \kappa_2^0(\omega)(x_2 + x_2^s - 2h)]} dk_1, \end{aligned} \quad (73)$$

$$F_2^0(k_1, \omega) = \frac{1}{\kappa_2^0(\omega)} \frac{-\mu^0 \kappa_2^0(\omega) \cos(K_2^1(\omega)h) - \mu^1 K_2^1(\omega) \sin(K_2^1(\omega)h)}{-\mu^0 \kappa_2^0(\omega) \cos(K_2^1(\omega)h) + \mu^1 K_2^1(\omega) \sin(K_2^1(\omega)h)}, \quad (74)$$

$$\begin{aligned} I_3^0(\mathbf{x}, \omega) &= \left[\int_{-\infty}^{-k^1} + \int_{k^1}^{\infty} \right] du_3^0(\mathbf{x}, \mathbf{x}_g, k_1, \omega) \\ &= \frac{S(\omega)}{4\pi} \left[\int_{-k^1}^{-k^0} + \int_{k^0}^{k^1} \right] F_3^0(k_1, \omega) e^{i[k_1(x_1 - x_1^s) - \kappa_2^0(\omega)(x_2 + x_2^s - 2h)]} dk_1, \end{aligned} \quad (75)$$

$$F_3^0(k_1, \omega) = \frac{1}{\kappa_2^0(\omega)} \frac{-\mu^0 \kappa_2^0(\omega) \cosh(\kappa_2^1(\omega)h) + \mu^1 \kappa_2^1(\omega) \sinh(\kappa_2^1(\omega)h)}{\kappa_2^0(\omega) - \mu^0 \kappa_2^0(\omega) \cosh(\kappa_2^1(\omega)h) - \mu^1 \kappa_2^1(\omega) \sinh(\kappa_2^1(\omega)h)}. \quad (76)$$

We write:

$$du_1^0(\mathbf{x}, \mathbf{x}_g, k_1, \omega) = G_1^0(\mathbf{x}_g, k_1, \omega) e^{i[k_1 x_1 + K_2^0(\omega) x_2]} dk_1, \quad (77)$$

$$G_1^0(\mathbf{x}_g, k_1, \omega) = \frac{S(\omega)}{4\pi} F_1^0(k_1, \omega) e^{-i[k_1 x_1^s - K_2^0(\omega)(x_2^s - 2h)]}, \quad (78)$$

which, together with (71), express the fact that a part (i.e. I_1^0) of the diffracted field in the half-space is composed of a sum of plane body waves (BW). Thus, to each horizontal wavenumber k_1 in the interval $[-k^0, k^0]$, correspond a SBW1 in Ω_1 and a BW in Ω_0^- .

In the same manner, we write:

$$du_2^0(\mathbf{x}, \mathbf{x}_g, k_1, \omega) = G_2^0(\mathbf{x}_g, k_1, \omega) e^{i k_1 x_1 - \kappa_2^0(\omega) x_2} dk_1, \quad (79)$$

$$G_2^0(\mathbf{x}_g, k_1, \omega) = \frac{S(\omega)}{4\pi} F_2^0(k_1, \omega) e^{-i k_1 x_1^s - \kappa_2^0(\omega)(x_2^s - 2h)}, \quad (80)$$

which, together with (73), express the fact that another part (i.e. I_2^0) of the diffracted field in the half-space is composed of a sum of plane surface waves (SW), henceforth denoted by SW2. Eq. (80) tells us that the amplitudes G_2^0 of the SW2 in I_2^0 decrease exponentially as the focal depth increases, so that the SW2 make themselves felt all the less the farther the source is (in the vertical direction) from the ground. On

the other hand, the amplitudes of the BW in I_1^0 are sinusoidal functions of focal depth, so that these BW can make themselves felt strongly for a large variety of source locations. In addition, we note that to each horizontal wavenumber k_1 in the intervals $[-k^1, -k^0]$ and $[k^0, k^1]$, correspond a SBW2 in Ω_1 and a SW2 in Ω_0^- .

Finally, we write:

$$du_3^0(\mathbf{x}, \mathbf{x}_g, k_1, \omega) = G_3^0(\mathbf{x}_g, k_1, \omega) e^{ik_1 x_1 - \kappa_2^0(\omega) x_2} dk_1, \quad (81)$$

$$G_3^0(\mathbf{x}_g, k_1, \omega) = \frac{S(\omega)}{4\pi} F_3^1(k_1, \omega) e^{-ik_1 x_1^s - \kappa_2^0(\omega)(x_2^s - 2h)}, \quad (82)$$

which, together with (75), express the fact that the third part (i.e. I_3^0) of the diffracted field in the substratum is composed of a sum of plane surface waves (henceforth denoted by SW3). Eq. (82) tells us that the amplitudes G_3^0 of the SW3 in I_3^0 decrease exponentially as the focal depth (i.e. $h + x_2^s$) increases, so that the SW3 make themselves felt all the less the farther the source is (in the vertical direction) from the ground. Note however, that the wavevectors associated with the SW3 are not identical to those associated with the SW2 because k_1 spans an interval in I_3^0 that is different from the one in I_2^0 . In addition, we note that to each horizontal wavenumber k_1 in the intervals $]-\infty, -k^1]$ and $[k^1, \infty[$, correspond a SSW in Ω_1 and a SW3 in Ω_0^- .

The main conclusion of this discussion is that for focal depths of the source that are sufficiently large, the frequency-domain response in the half-space is essentially given by I_1^0 and is expressed by a sum of BW. This corresponds more or less to the situation in the quasi-1-D analysis of the forward-scattering problem, but, as we shall see further on, it is, by no means, a valid picture of the response of the configuration when the focal depth of the source is not large.

5.3 Amplitudes of the SBW1

Henceforth, we restrict our attention to the field in the soft layer, and, in particular, to the three individual types of standing waves (SBW1, SBW2, SSW) of which it is composed. Here, we focus on a generic SBW1 and note that its amplitude G_1^1 is the product of three factors: the factor $S(\omega)$ associated with the spectrum of the incident pulse, a geometric factor associated with the location of the source (whose influence was already discussed), and a so-called *interference factor* F_1^1 . We first discuss the interference factor and then close the discussion with some remarks on $S(\omega)$.

We rewrite I_1^1 as

$$I_1^1(\mathbf{x}, \omega) = \frac{-S(\omega)}{\pi} \int_0^{k^0} F_1^1(k_1, \omega) \cos(k_1(x_1 - x_1^s)) \cos(K_2^1(\omega)x_2) e^{-iK_2^0(\omega)(h-x_2^s)} dk_1. \quad (83)$$

We make the change of variables

$$\eta = k^0 h = h \frac{\omega}{c^0}, \quad \zeta = \frac{k_1}{k^0}, \quad (84)$$

and adopt the definitions:

$$\nu = \frac{\mu^1}{\mu^0}, \quad \gamma = \frac{k^1}{k^0} = \frac{c^0}{c^1}, \quad \psi = \sqrt{1 - \zeta^2} \quad \phi = \sqrt{\gamma^2 - \zeta^2}. \quad (85)$$

Note that $\gamma > 1$ and $\nu < 1$ due to previous assumptions. Then

$$I_1^1(\mathbf{x}, \omega) = \frac{-S(\omega)}{\pi} \int_0^1 E_1^1(\zeta, \eta) \cos\left(\zeta \eta \frac{(x_1 - x_1^s)}{h}\right) \cos\left(\phi \eta \frac{x_2}{h}\right) e^{-i\psi \eta \frac{(h-x_2^s)}{h}} d\zeta, \quad (86)$$

wherein

$$E_1^1(\zeta, \eta) := \frac{1}{i\psi \cos(\phi\eta) + \nu\phi \sin(\phi\eta)}. \quad (87)$$

We now examine E_1^1 in the interval $\zeta \in [0, 1]$. Since η and ζ are real, the denominator in E_1^1 cannot vanish; however, it does attain minima for certain values of these parameters. Let us consider ζ to be constant and inquire for what values of η

$$|E_1^1(\zeta, \eta)|^{-2} = \psi^2 \cos^2(\phi\eta) + \nu^2 \phi^2 \sin^2(\phi\eta), \quad (88)$$

attains its minima. A necessary condition is:

$$\partial_\eta (|E_1^1(\zeta, \eta)|^{-2}) = 0 = \phi(\nu^2 \phi^2 - \psi^2) \sin(2\phi\eta). \quad (89)$$

There exist three possibilities, the first one of which is $\phi = 0$, but this implies $\zeta = \gamma > 1$ which is in contradiction with the fact ζ must lie in $[0, 1]$. The second possibility is that $\psi = \nu\phi$; we will reconsider this case further on. The third possibility is $\sin(2\phi\eta) = 0$ whence $\phi\eta = n\pi/2$; $n = 0, 1, \dots$. To determine for what values of n these roots correspond to actual minima of $|F_1^1(\zeta, \eta)|^{-2}$ we must have

$$\partial_\eta^2 (|F_1^1(\zeta, \eta)|^{-2})|_{\phi\eta=\frac{n\pi}{2}} = 2\phi^2(\nu^2\phi^2 - \psi^2)\cos(n\pi) > 0. \tag{90}$$

This condition gives rise to two types of solutions depending on the sign of $\nu^2\phi^2 - \psi^2$. The first type, which we call *even body wave* solutions (designated by the superscript *Be*) is:

$$\eta = \eta_m^{Be} = \frac{m\pi}{\phi}; \quad m = 0, 1, 2, \dots, \text{ when } \nu\phi > \psi. \tag{91}$$

The second type, which we call *odd body wave* solutions (designated by the superscript *Bo*) is:

$$\eta = \eta_m^{Bo} = \frac{(2m+1)\pi}{2\phi}; \quad m = 0, 1, 2, \dots, \text{ when } \nu\phi < \psi. \tag{92}$$

Let ζ^B be the value of ζ for which $\nu\phi = \psi$. We find

$$\zeta^B = \sqrt{\frac{1 - \nu^2\gamma^2}{1 - \nu^2}}, \tag{93}$$

or

$$\zeta^B = \sqrt{1 - \frac{(\gamma^2 - 1)\nu^2}{1 - \nu^2}}, \tag{94}$$

from which it follows that $\zeta^B < 1$, this meaning that the second possibility (i.e. $\nu\phi = \psi$) is not contradictory with the constraint $\zeta \in [0, 1]$.

Thus, the three types of solutions leading to minima of E_1^1 are:

$$\text{for } \zeta > \zeta^B : \eta = \eta_m^{Be} = \frac{m\pi}{\phi}; \quad m = 0, 1, 2, \dots, \tag{95}$$

$$\text{for } \zeta = \zeta^B : \text{ all } \eta, \tag{96}$$

$$\text{for } \zeta < \zeta^B : \eta = \eta_m^{Bo} = \frac{(2m+1)\pi}{2\phi}; \quad m = 0, 1, 2, \dots \tag{97}$$

The meaning of all this is that $\|E_1^1\|$ has regularly spaced (in terms of η) maxima for all values of ζ , which is another way of saying that $\|E_1^1\|$ is a periodic function of η for all ζ . The period of this function is π/ϕ (even when $\zeta = \zeta^B$, because a constant is a periodic function with arbitrary period). However, the function takes different forms in the three cases (95)–(97). In fact,

- (i) for $\zeta > \zeta^B$: $\|E_1^1\|$ has maxima equal to $\psi^{-1} = \text{at } \eta = m\pi/\phi$ and minima equal to $(\nu\phi)^{-1}$ at $\eta = (2m+1)\pi/2\phi$,
- (ii) for $\zeta = \zeta^B$: $\|E_1^1\|$ is a constant equal to $\psi^{-1} = (\nu\phi)^{-1}$ at all η ,
- (iii) for $\zeta < \zeta^B$: $\|E_1^1\|$ has minima equal to ψ^{-1} at $\eta = m\pi/\phi$ and maxima equal to $(\nu\phi)^{-1}$ at $\eta = (2m+1)\pi/2\phi$.

A numerical example will help to give a measure of the relative importance of these three types of solutions. Recall that:

$$\nu = \frac{\mu^1}{\mu^0} = \frac{(c^1)^2\rho^1}{(c^0)^2\rho^0}, \tag{98}$$

so that

$$\nu\gamma = \nu\frac{c^0}{c^1} = \frac{c^1\rho^1}{c^0\rho^0}. \tag{99}$$

Let us choose parameters that might be pertinent in the context of topics (a) and (b): $c^0 = 1000 \text{ m s}^{-1}$, $\rho^0 = 1500 \text{ kg m}^{-3}$, $c^1 = 100 \text{ m s}^{-1}$, $\rho^1 = 1000 \text{ kg m}^{-3}$, for which $\nu = 0.67 \times 10^{-2}$ and $\nu\gamma = 0.67 \times 10^{-1}$, whence $\zeta^B = 0.995$. Thus, $\|E_1^1\|$ takes the form of the type (iii) function in most of the interval $[0, 1]$, in fact in $0 \leq \zeta < 0.995$. In particular, for body waves whose wavevectors are nearly vertical (i.e. $0 \leq \zeta \ll 1$), the maximum of $\|E_1^1\|$ is

$$(\nu\phi)^{-1} = \frac{1}{\nu\sqrt{\gamma^2 - \zeta^2}} \approx \frac{1}{\nu\gamma} = \frac{c^0\rho^0}{c^1\rho^1}, \tag{100}$$

which, in the present numerical example, is equal to 15.

The lowest frequency ($\nu = \omega/2\pi$) for which this value is attained (obtained from $\eta = \pi/2\phi \approx \pi/2\gamma$) is

$$\nu = \frac{c^1}{4h}, \tag{101}$$

and is often called either the ‘fundamental Haskell resonance frequency’ (Bard & Bouchon 1980) or the ‘1-D resonance frequency’ (Bard & Bouchon 1985; Semblat *et al.* 2000) of the soft soil layer/hard substratum configuration. However, a sinusoidal response function of the type E_1^1 is not consistent with resonant response (which is large at the resonance frequencies in the absence of a dissipation mechanism) which would arise, for instance, in the context of excitation of some sort of structural mode; in fact, this sinuoidal response results from interference

of waves, which is the reason why we termed F_1^1 the ‘interference factor’. Thus, it is questionable whether it is appropriate to employ the term ‘resonances’ (Bard 1985; Bard & Bouchon 1980, 1985) in connection with body wave response (embodied in I_1^1) of the configuration.

To conclude this discussion, we now consider the spectral factor $S(\omega)$. It is obvious that if $S(\omega) = S(\eta c^0/h)$ is significantly large near the frequencies $\eta = (2m + 1)\pi/2\phi$; $m = 0, 1, \dots$, at which F_1^1 is large, then the product of these two functions, embodied in I_1^1 will be large at these frequencies. In particular, if $S(\omega) = S(\eta c^0/h)$ is maximal near the low frequency $\eta = \pi/2\phi$, then the response will be large over a large range of horizontal wavenumbers due to the contribution of the $m = 0$ maximum of the interference factor E_1^1 . This has been noted repeatedly in the past (Bard 1985; Bard & Bouchon 1980, 1985), and termed a ‘resonant response’, although (as pointed out in the preceding paragraph) $\eta = (2m + 1)\pi/2\phi$; $m = 0, 1, \dots$ are not resonance frequencies.

5.4 Amplitudes of the SBW2

We now direct our attention to the SBW2 component of the field in the soft layer. We note that the amplitude G_2^1 of the generic SBW2 is the product of three factors: the factor $S(\omega)$ associated with the spectrum of the incident pulse, a geometric factor associated with the location of the source (whose influence was already discussed), and a so-called interference factor $F_2^1 dk_1$. Here we discuss the product of the interference factor with $S(\omega)$ in order to evaluate the contribution of generic SBW2 to the overall response in the layer and on the ground.

We rewrite I_2^1 as

$$I_2^1(\mathbf{x}, \omega) = \frac{-S(\omega)}{\pi} \int_{k_0}^{k_1} F_2^1(k_1, \omega) \cos(k_1(x_1 - x_1^s)) \cos(K_2^1(\omega)x_2) e^{k_2^0(\omega)(h-x_2^s)} dk_1, \quad (102)$$

and make the same change of variables as in the previous section, employing the additional definition

$$\theta := \sqrt{\zeta^2 - 1}. \quad (103)$$

Thus

$$I_2^1(\mathbf{x}, \omega) = \frac{-S(\omega)}{\pi} \int_1^\gamma E_2^1(\zeta, \eta) \cos\left(\zeta \eta \frac{(x_1 - x_1^s)}{h}\right) \cos\left(\theta \eta \frac{x_2}{h}\right) e^{-\theta \eta (x_2^s - h)} d\zeta, \quad (104)$$

wherein

$$E_2^1(\zeta, \eta) := \frac{1}{-\theta \cos(\phi\eta) + \nu\phi \sin(\phi\eta)}. \quad (105)$$

Let us examine E_2^1 in the interval $\zeta \in [1, \gamma]$. Contrary to the previous case, here the denominator (in E_2^1) can vanish for real η and ζ , that is, $-\theta \cos(\phi\eta) + \nu\phi \sin(\phi\eta) = 0$,

$$(106)$$

this being none other than the *dispersion relation of Love modes*. The roots of this relation are:

$$\eta = \frac{1}{\phi} \left[\arctan\left(\frac{\theta}{\nu\phi}\right) + m\pi \right]; \quad m = 0, 1, 2, \dots, \quad (107)$$

wherein the arctan function is defined in $[-\pi/2, \pi/2]$ and can be expressed either by the series

$$\arctan y = y + \sum_{l=1}^{\infty} (-1)^l \frac{y^{2l+1}}{2l+1}; \quad y^2 < 1, \quad (108)$$

or by the series

$$\arctan y = \frac{\pi}{2} - \sum_{l=0}^{\infty} (-1)^l \frac{y^{-(2l+1)}}{2l+1}; \quad y^2 > 1. \quad (109)$$

It is easily shown that $\theta = \nu\phi$ when

$$\zeta = \zeta^L := \sqrt{1 + (\gamma^2 - 1) \frac{\nu^2}{1 + \nu^2}}, \quad (110)$$

so that $\zeta^L > 1$, as it should be for the constraint $\zeta \in [1, \gamma]$ to be satisfied.

Thus, three types of solutions lead to a zero in the denominator of F_2^1 : for:

$$\zeta < \zeta^L : \eta = \eta_m^{Le} = \frac{m\pi}{\phi} + \frac{1}{\phi} \left[\frac{\theta}{\nu\phi} - \frac{1}{3} \left(\frac{\theta}{\nu\phi} \right)^3 + \dots \right], \quad (111)$$

for:

$$\zeta = \zeta^L : \eta = \eta_m^L = \frac{(4m+1)\pi}{4\phi}, \quad (112)$$

for:

$$\zeta > \zeta^L : \eta = \eta_m^{Lo} = \frac{(2m+1)\pi}{2\phi} + \frac{1}{\phi} \left[-\frac{\nu\phi}{\theta} + \frac{1}{3} \left(\frac{\nu\phi}{\theta} \right)^3 + \dots \right], \quad (113)$$

and correspond to the existence of three types (even, neutral, odd) of Love modes whose eigenfrequencies are η_m^{Le} , η_m^L and η_m^{Lo} respectively.

This means that $\|E_2^1\|$ has regularly spaced (in terms of η) maxima for all values of ζ , which is another way of saying that $\|E_2^1\|$ is a periodic function of η for all ζ . The period of this function is π/ϕ (even when $\zeta = \zeta^L$ because a constant is a periodic function with arbitrary period). However, the function takes different forms in the three cases (111–113). In fact,

- (i) for $\zeta < \zeta^L$: $\|E_2^1\|$ has maxima equal to ∞ at $\eta = \eta_m^{Le}$,
- (ii) for $\zeta = \zeta^L$: $\|E_2^1\|$ has maxima equal to ∞ at $\eta = \eta_m^L$,
- (iii) for $\zeta > \zeta^L$: $\|E_2^1\|$ has minima equal to ∞ at $\eta = \eta_m^{Lo}$.

A numerical example will help give a measure of the relative importance of these three types of solutions. Let us again choose: $c^0 = 1000 \text{ m s}^{-1}$, $\rho^0 = 1500 \text{ kg m}^{-3}$, $c^1 = 100 \text{ m s}^{-1}$, $\rho^1 = 1000 \text{ kg m}^{-3}$, for which $\gamma = 10$, $\nu = 0.67 \times 10^{-2}$ and $\nu\gamma = 0.67 \times 10^{-1}$, whence $\zeta^L = 1.0044$. Thus, $|F_2^1|$ takes the form of the type (iii) function for most of the interval $[1, \gamma]$, in fact in $1.0044 \leq \zeta < 10$.

A few remarks are in order.

(1) contrary to what may be inferred from works such as Bard & Bouchon (1980, 1985), Bard (1985) and Chávez-García & Bard (1994), the individual Love modes do not have the structure of surface waves in the layer (and, therefore, on the ground) since the SBW2 are actually standing body waves; the only feature they share with surface waves (i.e. the SW that coexist in the hard substratum when Love modes are excited) is their phase velocity

$$c^L = \frac{c^0}{\zeta}, \quad (114)$$

wherein it can be noted that due to the fact that $\zeta \in [1, \gamma]$,

$$c^L < c^0, \quad (115)$$

which means that the phase velocity of Love modes (shared by the SBW2 in the layer and the SW in the hard substratum) is less than the phase velocity of body waves in the hard substratum,

(2) contrary to what occurs in connection with the SBW1, the excitation of Love modes is indeed a resonant process, because Love modes are actually structural modes of the soft layer/hard substratum configuration and because the response associated with each of these modes is large at resonance in the absence of dissipation in both of the media of the configuration and

(3) the resonant frequencies of the Love modes are not identical to the frequencies at which the SBW1 attain their maxima; for instance, the difference of these frequencies, for the m th prevalent odd-type SBW1 and SBW2, is:

$$\eta_m^{Bo} - \eta_m^{Lo} = \frac{1}{\phi} \left[\frac{\nu\phi}{\theta} - \frac{1}{3} \left(\frac{\nu\phi}{\theta} \right)^3 + \dots \right], \quad (116)$$

which means that the frequency of occurrence of the maxima of the m th order SBW1 is higher than (although it can be close to) that of the corresponding SBW2 (note that the difference in (116) does not depend on m).

To conclude this discussion, we again consider the spectral factor $S(\omega)$. It is obvious that if $S(\omega) = S(\eta c^0/h)$ is significantly large near the frequencies η_m^{Lo} at which E_2^1 is large (infinite if no dissipation is present), then the product of these two functions, embodied in I_2^1 , will be large at these frequencies. In particular, if $S(\eta c^0/h)$ is maximal near the low frequency η_0^{Lo} , then the response will be large over a large range of horizontal wavenumbers. If $S(\omega) = S(\eta c^0/h)$ is maximal near the low frequency η_0^{Lo} , and η_0^{Lo} is not too far from η_0^{Bo} , then the global response can be even larger due to the cumulative contribution of both the SBW1 and SBW2.

5.5 Amplitudes of the SSW

We direct our attention to the SSW component of the field in the soft layer. We note that the amplitude G_3^1 of the generic SSW is the product of three factors: $S(\omega)$ which is associated with the spectrum of the incident pulse, a geometric factor associated with the location of the source (whose influence was already discussed), and the interference factor F_3^1 . Here we discuss the product of the interference factor with $S(\omega)$ in order to evaluate the contribution of generic SSW to the overall response in the layer and on the ground.

We rewrite I_3^1 as

$$I_3^1(\mathbf{x}, \omega) = \frac{-S(\omega)}{\pi} \int_{k_1}^{\infty} E_3^1(k_1, \omega) \cos(k_1(x_1 - x_1^s)) \cosh(k_2^1(\omega)x_2) e^{k_2^0(\omega)(h-x_2^s)} dk_1, \quad (117)$$

and make the same change of variables as in the previous two sections, employing the additional definition

$$\chi := \sqrt{\zeta^2 - \gamma^2}, \quad (118)$$

so that

$$I_3^1(\mathbf{x}, \omega) = \frac{-S(\omega)}{\pi} \int_{\gamma}^{\infty} E_3^1(\zeta, \eta) \cos\left(\zeta \eta \frac{(x_1 - x_1^s)}{h}\right) \cosh\left(\chi \eta \frac{x_2}{h}\right) e^{-\theta \eta (x_2^s - h)} d\zeta, \quad (119)$$

wherein

$$E_3^1(\zeta, \eta) = \frac{-1}{\theta \cosh(\chi \eta) + \nu \chi \sinh(\chi \eta)}. \quad (120)$$

Since $\chi \geq 0$ for $\zeta \in [\gamma, \infty[$, and $\eta > 0$, $\sinh(\chi\eta) \geq 0$ and $\cosh(\chi\eta) > 0$ for $\zeta \in [\gamma, \infty[$, which means that the denominator in the previous formula cannot vanish for real η and ζ . It can however exhibit minima for $\zeta \in [\gamma, \infty[$.

Let us consider ζ to be constant and inquire for what values of η the denominator E_3^1 has minima. This requires that

$$\partial_\eta (|E_3^1(\zeta, \eta)|^{-1}) = -\chi [\theta \sinh(\chi\eta) + \nu \chi \cosh(\chi\eta)] = 0. \quad (121)$$

However, $[\] \neq 0$ except for $\chi = 0$, i.e. for $\zeta = \gamma$ and $\forall \eta$. When $\chi = 0$ we find $|E_3^1|^{-1} = \theta$, and from the fact that $\sinh(\chi\eta) \geq 0$ and $\theta \cosh(\chi\eta) \geq \theta$ for $\zeta \in [\gamma, \infty[$, we conclude that $|E_3^1|^{-1} \geq \theta$. This means that $\zeta = \gamma$ corresponds to the location of a minimum of $|E_3^1|^{-1}$ and this holds for all η .

Thus, $|E_3^1|$ is a monotonically decreasing function of ζ for all $\zeta \in]\gamma, \infty[$ and attains its maximum equal to $\theta^{-1} = 1/\sqrt{\gamma^2 - 1}$ at $\zeta = \gamma$ for all η .

To get an idea of the magnitude of this function, notably in relation to E_1^1 , we again consider the numerical example: $c^0 = 1000 \text{ m s}^{-1}$, $\rho^0 = 1500 \text{ kg m}^{-3}$, $c^1 = 100 \text{ m s}^{-1}$, $\rho^1 = 1000 \text{ kg m}^{-3}$, for which $\gamma = 10$, whence $\max \|E_3^1\| \leq 0.1005$ which is much less than $\max \|E_1^1\| = 15$ for the same set of parameters.

Since the maximum of E_3^1 is attained at all frequencies (i.e. for all η), the spectrum function $S(\omega)$ does not influence the relative contribution of I_3^1 to the ground response. Thus, to conclude this discussion, we can say that the SSW contribute relatively little to the ground response in comparison to the SBW1 and SBW2, except perhaps at frequencies close to the minima of the functions E_1^1 and E_2^1 .

6 THE POLE-BRANCH CUT REPRESENTATION OF THE SPECTRA OF THE TOTAL FIELD IN THE LAYER AND OF THE DIFFRACTED FIELD IN THE HALF-SPACE

This subject matter is treated in more detail in Appendix B of the companion paper (Groby & Wirgin 2005). Here, we present only the main features, assuming, once again, that the media filling the layer and half-space are free of dissipation and that $k^1 > k^0$.

We can rewrite (50)–(51) as follows (taking into account (40):

$$u^{0d}(\mathbf{x}, \omega) = S(\omega) \int_{-\infty}^{\infty} \left[\frac{N^0(k_1, \omega)}{D(k_1, \omega)} \right] e^{i[k_1(x_1 - x_1^*) + k_2^0(\omega)(x_2 + x_2^* - 2h)]} dk_1; \quad \forall \mathbf{x} \in \Omega_0, \quad (122)$$

$$u^1(\mathbf{x}, \omega) = u^{1d}(\mathbf{x}, \omega) = S(\omega) \int_{-\infty}^{\infty} \left[\frac{N^1(k_1, \omega)}{D(k_1, \omega)} \right] \cos(k_2^1(\omega)x_2) e^{i[k_1(x_1 - x_1^*) - k_2^0(\omega)(h - x_2^*)]} dk_1; \quad \forall \mathbf{x} \in \Omega_1, \quad (123)$$

wherein

$$N^0(k_1, \omega) := \frac{i}{4\pi k_2^0(\omega)} [i\mu^0(\omega)k_2^0(\omega) \cos(k_2^1(\omega)h) - \mu^1(\omega)k_2^1(\omega) \sin(k_2^1(\omega)h)], \quad (124)$$

$$N^1(k_1, \omega) := \frac{i}{4\pi k_2^0(\omega)} [2i\mu^0(\omega)k_2^0(\omega)], \quad (125)$$

$$D(k_1, \omega) := i\mu^0(\omega)k_2^0(\omega) \cos(k_2^1(\omega)h) + \mu^1(\omega)k_2^1(\omega) \sin(k_2^1(\omega)h). \quad (126)$$

The material in Section 5.4 indicates that $D(k_1, \omega)$ can vanish at a denumerable set of real values of k_1 (the resonance wavenumbers of the Love modes) in the interval $[k^0, k^1]$. Assume that the frequency is such (i.e. is low) that only one such value exists and call it k_1^* . Then the integrands in (122)–(123) are singular for $k_1 = k_1^*$, which suggests that the corresponding integrals be evaluated with the help of Cauchy's theorem (Whittaker & Watson 1922; Carrier *et al.* 1983).

Consider the first of these two integrals. To apply Cauchy's theorem, we evaluate an auxiliary closed contour (this contour is described in Appendix B of Groby & Wirgin (2005)) integral having the same integrand as the previous one, whose contour comprises the real k_1 axis and suitable branch lines extending from the branch point $k_1 = k^0$ to $k_1 = \pm i\infty$. Cauchy's theorem tells us that the auxiliary closed-contour integral equals $2\pi i$ times the residue of the pole located within the integration path, so that, due to the fact that the contribution of the integral along the semi-circle of infinite radius is nil, one finds

$$u^{0d}(\mathbf{x}, \omega) = 2\pi i S(\omega) \left[\frac{N^0(k_1^*, \omega)}{\dot{D}(k_1^*, \omega)} \right] \times e^{i[k_1^*(x_1 - x_1^*) - k_2^{0*}(\omega)(x_2 + x_2^* - 2h)]} + u_{\mathcal{B}}^{0d}(\mathbf{x}, \omega); \quad \forall \mathbf{x} \in \Omega_0, \quad (127)$$

wherein

$$k_2^{0*}(\omega) := i\kappa_2^{0*} = i \left\| \sqrt{(k_1^*)^2 - (k^0(\omega))^2} \right\|$$

$$k_2^{1*}(\omega) := K_2^{1*} = \left\| \sqrt{(k^1(\omega))^2 - (k_1^*)^2} \right\|, \quad (128)$$

$$\dot{D}(k_1^*, \omega) := \left. \frac{\partial D(k_1, \omega)}{\partial k_1} \right|_{k_1=k_1^*}, \quad (129)$$

and $u_B^{0d}(\mathbf{x}, \omega)$ is the contribution from the branch cut integrals (see Appendix B of Groby & Wirgin 2005, for the full expressions of these integrals).

Proceeding in the same manner for u^1 results in

$$u^1(\mathbf{x}, \omega) = 2\pi i S(\omega) \frac{1}{4\pi \kappa_2^{0*}(\omega)} \left[\frac{N^1(k_1^*, \omega)}{D(k_1^*, \omega)} \right] \times \cos(K_2^{1*}(\omega)x_2) e^{[i k_1^*(x_1 - x_1^*) + \kappa_2^{0*}(\omega)(h - x_2^2)]} + u_B^1(\mathbf{x}, \omega); \quad \forall \mathbf{x} \in \Omega_1. \quad (130)$$

Remark 1 The pole contribution to u^{0d} (first term on the right hand side of (127)) has the structure of a (type SW2) *surface wave* whose wavenumber k_1^* is that of the fundamental Love mode.

Remark 2 The amplitude of this pole contribution to u^{0d} is all the larger, the smaller is the distance of the source from the lower boundary of the layer (recall that the source was assumed to lie in the lower half-space).

Remark 3 The pole contribution to u^1 (first term on the right-hand side of (130)) has the structure of a (type SBW2) *standing bulk wave* whose wavenumber k_1^* is that of the fundamental Love mode.

Remark 4 The amplitude of this pole contribution to u^1 is all the larger, the smaller is the distance of the source from the lower boundary of the layer.

Remark 5 We have not given an explicit expression to the branch cut contributions u_b^{0d} to u^{0d} and u_b^1 to u^1 , but it is shown in Groby & Wirgin (2005) that these are all the smaller, with respect to the pole contribution, the larger is the hypocentral distance; thus, for all but perhaps very small hypocentral distances, the frequency-domain ground response is dominated by the Love mode contribution, whereas at small hypocentral distances it is possible for something else to interfere with the Love modes. This ‘something else’ was associated with the so-called Haskell ‘modes’ in the SBW1+SBW2+SSW representation of Section 5. We shall give a more accurate appraisal of their influence in the companion paper (Groby & Wirgin 2005).

7 COMMENTS ON THE THE SBW1+SBW2+SSW AND POLE+BRANCH CUT REPRESENTATIONS OF THE GROUND RESPONSE

Although the theoretical analysis carried out in Section 5 may be useful for underlining the role played by the different types of body and surface waves that appear in the fields in the layer and substratum, it does not resolve the practical problem of the actual evaluation of the integrals I_1^1 , I_2^1 and I_3^1 for the frequency-domain ground response. Another apparent drawback of this analysis is that it was restricted to the case in which the layer is elastic, but the conclusions that were drawn for the elastic layer case should not be radically different for the case of a weakly or moderately viscoelastic layer.

Although the analysis of Section 6 leads to an apparently simple result (i.e. for the pole contributions), in point of fact we are generally faced with the problem of evaluating the branch cut integrals.

Consequently, we resort, in the companion paper (Groby & Wirgin 2005), to a purely numerical approach for the evaluation of I_1^1 , I_2^1 and I_3^1 and of their sum to determine the frequency-domain response on the ground of the layer/substratum configuration. Since physically realistic configurations involve viscoelastic layers, we evaluate these integrals and the total frequency response $u(\mathbf{x}_g, \omega)$ under the assumption of viscoelastic layers. Once $u(\mathbf{x}_g, \omega)$ are computed, we determine the temporal signal $u(\mathbf{x}_g, t)$, again by purely numerical means, via (34).

In Groby & Wirgin (2005) we also evaluate numerically the roots of the dispersion relation of Love modes to determine the pole contributions as well as the branch cut integrals for both elastic and viscoelastic layers. We subsequently proceed, as in the previous paragraph, to obtain the time history of ground response from the spectrum of this response, embodied in the sum of the pole and branch cut terms.

The weakness of these essentially numerical approaches lies in the difficulty of discerning the mechanisms underlying the observed *time history* of ground response. To overcome this drawback, we develop, in the next section (Section 8), an analysis for obtaining the time history in direct manner which appears to facilitate the comprehension of particular features of the time histories of ground response.

8 DIRECT ANALYSIS OF THE TIME HISTORY OF GROUND RESPONSE

Before going into the details of this analysis, we stress the facts that: (i) the layer is generally anelastic, and (ii) the layer is softer than the substratum, which, at present, means that μ^1 and c^1 are generally complex and

$$\|\mu^1\| < \|\mu^0\|, \quad \|c^1\| < \|c^0\|. \quad (131)$$

8.1 General features of the time-domain response on the ground

The point of departure is (34) wherein we make the change of variables described in (84) and (85).

The time-domain ground response becomes

$$u^1(\mathbf{x}_g, t) = 2 \frac{c^0}{h} \Re \int_0^\infty u^1 \left(\mathbf{x}_g, \eta \frac{c^0}{h} \right) e^{-i\eta \frac{c^0}{h} t} d\eta, \quad (132)$$

with, by virtue of (52),

$$u^1\left(\mathbf{x}_g, \eta \frac{c^0}{h}\right) = -\frac{S\left(\frac{c^0}{h}\eta\right)}{2\pi} \int_{-\infty}^{\infty} [i\alpha(\zeta) \cos(\eta\beta(\zeta)) + \nu\beta(\zeta) \sin(\eta\beta(\zeta))]^{-1} \\ \times e^{i\eta\left[\frac{(x_1-x_1^*)}{h}\zeta + \frac{(x_2^2-h)}{h}\alpha(\zeta)\right]} d\zeta; \quad \forall x_1 \in \mathbb{R}, \quad (133)$$

in which:

$$\alpha(\zeta) := \sqrt{1-\zeta^2}; \quad \Re\alpha \geq 0, \quad \Im\alpha \geq 0, \quad (134)$$

$$\beta(\zeta) := \sqrt{\gamma^2-\zeta^2}; \quad \Re\beta \geq 0, \quad \Im\beta \geq 0. \quad (135)$$

Note that on account of (131),

$$\|v\| < 1, \quad \|\gamma\| > 1. \quad (136)$$

Changing the orders of integration in (132) and (133) gives

$$u^1(\mathbf{x}_g, t) = -\frac{c^0}{\pi h} \int_{-\infty}^{\infty} J^1(\mathbf{x}_g, t, \zeta) d\zeta, \quad (137)$$

wherein

$$J^1(\mathbf{x}_g, t, \zeta) = \Re \int_0^{\infty} S\left(\frac{c^0}{h}\eta\right) [i\alpha(\zeta) \cos(\eta\beta(\zeta)) + \nu\beta(\zeta) \sin(\eta\beta(\zeta))]^{-1} \\ \times e^{i\eta\left[\frac{(x_1-x_1^*)}{h}\zeta + \frac{(x_2^2-h)}{h}\alpha(\zeta) - \frac{c^0}{h}t\right]} d\eta. \quad (138)$$

We note from (134) that α is real for $|\zeta| < 1$ and imaginary for $|\zeta| > 1$, or, in other words:

$$\alpha(\zeta) := \psi(\zeta) = |\sqrt{1-\zeta^2}|; \quad |\zeta| < 1, \quad (139)$$

$$\alpha(\zeta) := i\theta(\zeta) = i|\sqrt{\zeta^2-1}|; \quad |\zeta| > 1. \quad (140)$$

For future use, we define:

$$\beta(\zeta) = i\chi(\zeta) = i\sqrt{\zeta^2-\gamma^2}, \quad (141)$$

with

$$\chi(\zeta) := \sqrt{\zeta^2-\gamma^2}. \quad (142)$$

Thus

$$u^1(\mathbf{x}_g, t) = -\frac{c^0}{\pi h} \left[\int_{-1}^1 J_1^1(\mathbf{x}_g, t, \zeta) d\zeta + \left\{ \int_{-\Re\gamma}^{-1} + \int_1^{\Re\gamma} \right\} J_2^1(\mathbf{x}_g, t, \zeta) d\zeta \right. \\ \left. + \left\{ \int_{-\infty}^{-\Re\gamma} + \int_{\Re\gamma}^{\infty} \right\} J_3^1(\mathbf{x}_g, t, \zeta) d\zeta \right] = u_1^1(\mathbf{x}_g, t) + u_2^1(\mathbf{x}_g, t) + u_3^1(\mathbf{x}_g, t), \quad (143)$$

wherein

$$J_1^1(\mathbf{x}_g, t, \zeta) = \Re \int_0^{\infty} S\left(\frac{c^0}{h}\eta\right) \mathcal{D}_1^{-1}(\zeta, \eta) e^{i\eta\left[\frac{(x_1-x_1^*)}{h}\zeta + \frac{(x_2^2-h)}{h}\psi(\zeta) - \frac{c^0}{h}t\right]} d\eta, \quad (144)$$

$$J_2^1(\mathbf{x}_g, t, \zeta) = \Re \int_0^{\infty} S\left(\frac{c^0}{h}\eta\right) \mathcal{D}_2^{-1}(\zeta, \eta) e^{i\eta\left[\frac{(x_1-x_1^*)}{h}\zeta + i\frac{(x_2^2-h)}{h}\theta(\zeta) - \frac{c^0}{h}t\right]} d\eta, \quad (145)$$

$$J_3^1(\mathbf{x}_g, t, \zeta) = \Re \int_0^{\infty} S\left(\frac{c^0}{h}\eta\right) \mathcal{D}_3^{-1}(\zeta, \eta) e^{i\eta\left[\frac{(x_1-x_1^*)}{h}\zeta + i\frac{(x_2^2-h)}{h}\theta(\zeta) - \frac{c^0}{h}t\right]} d\eta, \quad (146)$$

with:

$$\mathcal{D}_1(\zeta, \eta) := i\psi(\zeta) \cos(\eta\beta(\zeta)) + \nu\beta(\zeta) \sin(\eta\beta(\zeta)), \quad (147)$$

$$\mathcal{D}_2(\zeta, \eta) := -\theta(\zeta) \cos(\eta\beta(\zeta)) + \nu\beta(\zeta) \sin(\eta\beta(\zeta)), \quad (148)$$

$$\mathcal{D}_3(\zeta, \eta) := -\theta(\zeta) \cosh(\eta\chi(\zeta)) - \nu\chi(\zeta) \sinh(\eta\chi(\zeta)). \quad (149)$$

8.1.1 *Complex zeros of \mathcal{D}_1*

Let us first consider \mathcal{D}_1 in which: ζ and ψ are real, whereas ν and β are generally complex due to the fact that μ^1 and k^1 (and consequently γ) are generally complex (because the layer is generally dissipative).

We search for the *complex* roots

$$\eta = \eta^B := \eta'^B + i\eta''^B \quad (150)$$

of the equation

$$\mathcal{D}_1(\zeta, \eta^B) = 0; \quad \zeta \in [-1, 1]. \quad (151)$$

The reason for assigning the superscript ‘B’ will become apparent further on. With the definitions:

$$a^B := \Re(\eta^B \beta(\zeta)), \quad b^B := \Im(\eta^B \beta(\zeta)), \quad c := \Re(\nu\beta(\zeta)), \quad d := \Im(\nu\beta(\zeta)), \quad (152)$$

the real and imaginary parts of (151) yield

$$\psi \sin a^B \sinh b^B + c \sin a^B \cosh b^B - d \cos a^B \sinh b^B = 0, \quad (153)$$

$$\psi \cos a^B \cosh b^B + c \cos a^B \sinh b^B + d \sin a^B \cosh b^B = 0, \quad (154)$$

which constitutes a coupled system of two non-linear equations in the two unknowns a^B, b^B .

One can show that these two equations imply

$$b^B \leq 0. \quad (155)$$

Remark 1 In the *non-dissipative* case, ν and γ are real, and β is real due to eqs (135) and (136) and to the fact that $|\zeta| \leq 1$, so that $d = 0$ and (153)–(154) yield

$$\psi \sin a^B \cos a^B = 0. \quad (156)$$

This is the relation defining the wavenumbers of the so-called Haskell ‘modes’, called SBW1 in Section 5, which we showed take the form of body (B) waves in the substratum and layer. This is the reason why the superscript B was attached to the roots of (153)–(154). It was shown in Section 5.3 that the so-called *even* solutions of (156) are

$$\sin a^B = 0 \Rightarrow a^B = a_m^{Be} = m\pi; \quad m = 0, 1, 2, \dots, \quad (157)$$

and the so-called *odd* solutions of (156) are

$$\cos a^B = 0 \Rightarrow a^B = a_m^{Bo} = \frac{2m+1}{2}\pi; \quad m = 0, 1, 2, \dots, \quad (158)$$

whence

$$\eta'^B = \eta_m^{Be} = \frac{a_m^{Be}}{\beta} = \frac{m\pi}{\beta}; \quad m = 0, 1, 2, \dots, \quad \text{when } \psi < c, \quad (159)$$

$$\eta'^B = \eta_m^{Bo} = \frac{a_m^{Bo}}{\beta} = \frac{(2m+1)\pi}{2\beta}; \quad m = 0, 1, 2, \dots, \quad \text{when } \psi > c. \quad (160)$$

Furthermore, the fact that $b^B < 0$ implies (since $b^B = \Im(\eta^B \beta)$ and β is real)

$$\eta''^{Be} = \Im(\eta^{Be}) < 0, \quad \eta''^{Bo} = \Im(\eta^{Bo}) < 0. \quad (161)$$

Remark 2 In the case of weak dissipation, the terms containing d in eqs (153) and (154) add a small perturbation to the Haskell ‘mode’ solutions.

Remark 3 This suggests, in the case in which the layer is *dissipative*, initializing the iterative scheme for obtaining η^B and η''^B , by their values of the non-dissipative case.

Remark 4 Note that it is not a^B and b^B that we are actually looking for, but rather η^B and η''^B . We have

$$a^B = \Re(\beta\eta^B) = \beta'\eta'^B - \beta''\eta''^B, \quad b^B = \Im(\beta\eta^B) = \beta'\eta''^B + \beta''\eta'^B, \quad (162)$$

which constitutes a set of two coupled equations for obtaining η^B and η''^B from a^B and b^B . This shows that it might be better to solve eqs (153) and (154) directly in terms of η^B and η''^B .

8.1.2 *Complex zeros of \mathcal{D}_2*

Let us next consider \mathcal{D}_2 in which: ζ and θ are real, whereas as before, ν and β are generally complex.

We search for the *complex* roots

$$\eta = \eta^L := \eta'^L + i\eta''^L \quad (163)$$

of the equation

$$\mathcal{D}_2(\zeta, \eta^L) = 0; \quad \zeta \in [-\Re\gamma, -1] \cup [1, \Re\gamma], \quad (164)$$

wherein the reason for assigning the superscript ‘ L ’ to solutions of (164) will become apparent further on. With the definitions:

$$a^L := \Re(\eta^L \beta(\zeta)), \quad b^L := \Im(\eta^L \beta(\zeta)), \quad (165)$$

and c and d as previously, the real and imaginary parts of (164) yield

$$-\theta \cos a^L \cosh b^L + c \sin a^L \cosh b^L - d \cos a^L \sinh b^L = 0, \quad (166)$$

$$\theta \sin a^L \sinh b^L + c \cos a^L \sinh b^L + d \sin a^L \cosh b^L = 0. \quad (167)$$

Once again, we are faced with the problem of solving a coupled system of two equations, now in terms of the unknowns a^L and b^L . As previously, we can show that

$$b^L \leq 0. \quad (168)$$

Remark 1 In the *non-dissipative* case, ν and γ are real, and β is real due to (135)–(136) and to the fact that, in the present case $\gamma \geq |\zeta| \geq 1$, so that we find from eqs (166) and (167)

$$-\theta \cos a^L + c \sin a^L = 0, \quad (169)$$

which is none other than the *dispersion relation of Love modes in the case of a non-dissipative layer in welded contact, and overlying, a non-dissipative substratum of half-infinite extent.*

One shows that another consequence of (166)–(167) is

$$b^L = 0 \Rightarrow \eta^{L'} = 0. \quad (170)$$

In other words, *the natural frequencies of Love modes in non-dissipative media are real.*

Proceeding as in Section 5.4 we find (in the absence of dissipation):

$$a^L := a_m^{Le} = m\pi + \left[\frac{\theta}{c} - \frac{1}{3} \left(\frac{\theta}{c} \right)^3 + \dots \right]; \quad m = 0, 1, 2, \dots; \quad \text{when } \frac{\theta}{c} < 1, \quad (171)$$

$$a^L := a_m^{Lo} = \frac{(2m+1)\pi}{2} + \left[- \left(\frac{\theta}{c} \right)^{-1} + \frac{1}{3} \left(\frac{\theta}{c} \right)^{-3} + \dots \right]; \quad m = 0, 1, 2, \dots; \quad \text{when } \frac{\theta}{c} > 1. \quad (172)$$

Remark 1 The terms involving d in eqs (166) and (167) add a small perturbation to the natural frequencies of the (even (e) and odd (o)) Love modes when account is taken of (small) dissipation.

Remark 2 See *Remark 4* of Section 8.1.1.

8.1.3 Complex zeros of D_3

Let us next consider \mathcal{D}_3 in which: ζ and θ are real, whereas ν and χ are generally complex.

We search for the *complex* roots

$$\eta = \eta^S := \eta'^S + i\eta''^S \quad (173)$$

of the equation

$$\mathcal{D}_3(\zeta, \eta^S) = 0; \quad \zeta \in]-\infty, -\Re\gamma] \cup [\Re\gamma, \infty[, \quad (174)$$

wherein the reason for assigning the superscript ‘ S ’ to solutions of (174) is to distinguish the latter from the ‘ B ’ and ‘ L ’ solutions.

With the definitions:

$$a^S := \Re(\eta^S \chi(\zeta)) \quad b^S := \Im(\eta^S \chi(\zeta)), \quad (175)$$

$$c := \Re(\nu \chi(\zeta)) \quad d := \Im(\nu \chi(\zeta)), \quad (176)$$

the real and imaginary parts of (174) yield

$$-\theta \cos b^S \cosh a^S - c \cos b^S \sinh a^S + d \sin b^S \cosh a^S = 0, \quad (177)$$

$$-\theta \sin b^S \sinh a^S - c \sin b^S \cosh a^S - d \cos b^S \sinh a^S = 0, \quad (178)$$

which constitutes a coupled system of two nonlinear equations for the two unknowns a^S and b^S . It can be shown that a consequence of these two equations is:

$$a^S \leq 0. \quad (179)$$

In the *non-dissipative* case, we obtain from (eqs 177 and 178) the two sets of solutions:

$$b^S := b_m^{Se} = m\pi, \quad a^S := a^{Se} = \operatorname{arctanh} \left(\frac{-\theta}{c} \right); \quad m = 0, 1, 2, \dots, \quad (180)$$

$$b^s := b_m^{s_0} = \frac{(2m+1)\pi}{2}, \quad a^s := a^{s_0} = \operatorname{arccoth}\left(\frac{-\theta}{c}\right); \quad m = 0, 1, 2, \dots \quad (181)$$

Remark 1 In the case in which there is a small amount of *dissipation*, the terms containing $d \neq 0$ in (177)–(178) constitute a small perturbation to the solutions (180)–(181), which fact suggests using the dissipationless solutions as starting solutions in an iterative scheme to obtain the solutions in the case in which there is dissipation.

Remark 2 See *Remark 4* of Section 8.1.1.

8.2 Specific features of the time-domain response on the ground

8.2.1 Approximate evaluation of an integral along the real axis of a function that has complex poles

We saw in Section that the time-domain response on the ground reduces to a sum of integrals of the type

$$J(\xi) := \int_0^\infty S\left(\frac{c^0 \eta'}{h}\right) \frac{\mathcal{N}(\xi, \eta')}{\mathcal{D}(\xi, \eta')} d\eta', \quad (182)$$

wherein: (i) η has been replaced by η' to stress the fact that this integration variable is *real*, and (ii) $\mathcal{N}(\xi, \eta')$ is of the generic form

$$\mathcal{N}(\xi, \eta') := e^{-i\eta' T(\xi)}. \quad (183)$$

The important point is that

$$\mathcal{D}(\xi, \eta) = 0 \quad \text{for } \eta =: \eta_m = \eta'_m + i\eta''_m; \quad m = 0, 1, 2, \dots, \quad (184)$$

it being understood that η_m is a generic designation for η_m^{Be} , η_m^{Bo} , η_m^{Le} , η_m^{Lo} , η_m^{Se} , and η_m^{So} . Eq. (184) suggests developing $\mathcal{D}(\xi, \eta)$ in a Taylor series around $\eta = \eta_m$, which gives

$$\mathcal{D}(\xi, \eta) = \mathcal{D}(\xi, \eta_m) + (\eta - \eta_m) \left. \frac{\partial \mathcal{D}(\xi, \eta)}{\partial \eta} \right|_{\eta=\eta_m} + \dots, \quad (185)$$

or, on account of (184):

$$\mathcal{D}(\xi, \eta') \approx (\eta' - \eta_m) \dot{\mathcal{D}}(\xi, \eta_m), \quad (186)$$

wherein

$$\dot{\mathcal{D}}(\xi, \eta_m) := \left. \frac{\partial \mathcal{D}(\xi, \eta)}{\partial \eta} \right|_{\eta=\eta_m}. \quad (187)$$

Consequently,

$$\begin{aligned} \|\mathcal{D}(\xi, \eta')\|^2 &\approx \|\eta' - \eta_m\|^2 \|\dot{\mathcal{D}}(\xi, \eta_m)\|^2 \\ &= [(\eta')^2 - 2\eta'\eta'_m + (\eta'_m)^2 + (\eta''_m)^2] \|\dot{\mathcal{D}}(\xi, \eta_m)\|^2 \\ &= [(\eta' - \eta'_m)^2 + (\eta''_m)^2] \|\dot{\mathcal{D}}(\xi, \eta_m)\|^2. \end{aligned} \quad (188)$$

It follows that

$$J(\xi) \approx \sum_{m=0}^\infty \int_{\eta^m}^{\eta^{m+1}} S\left(\frac{c^0 \eta'}{h}\right) \frac{\mathcal{N}(\xi, \eta')(\eta' - \eta'_m + i\eta''_m)}{\mathcal{D}(\xi, \eta_m)[(\eta' - \eta'_m)^2 + (\eta''_m)^2]} d\eta', \quad (189)$$

wherein $\eta^0 = 0$, η^1 , η^2 , \dots , are points on the η' axis such that $\eta^m = \frac{\eta'_m + \eta''_{m-1}}{2}$ which means that $\eta'_m \in [\eta^m, \eta^{m+1}]$; $m = 0, 1, 2, \dots$

Let $\mathcal{G}_m(\eta')$ be the Gaussian function

$$\mathcal{G}_m(\eta') := \frac{1}{\sqrt{\pi(\eta''_m)^2}} e^{-\frac{(\eta' - \eta'_m)^2}{(\eta''_m)^2}} = \frac{1}{\sqrt{\pi}} \frac{1}{\eta''_m} \frac{1}{e^{\frac{(\eta' - \eta'_m)^2}{(\eta''_m)^2}}}. \quad (190)$$

Expanding the exponential in a Taylor series gives

$$e^{-\frac{(\eta' - \eta'_m)^2}{(\eta''_m)^2}} = 1 + \frac{1}{1!} \frac{(\eta' - \eta'_m)^2}{(\eta''_m)^2} + \dots \approx \frac{1}{(\eta''_m)^2} [(\eta' - \eta'_m)^2 + (\eta''_m)^2], \quad (191)$$

so that

$$\mathcal{G}_m(\eta') \approx \frac{1}{\sqrt{\pi}} \frac{\eta''_m}{(\eta' - \eta'_m)^2 + (\eta''_m)^2}, \quad (192)$$

whence

$$J(\xi) \approx \sum_{m=0}^\infty \frac{\sqrt{\pi}}{\eta''_m} \frac{1}{\dot{\mathcal{D}}(\xi, \eta_m)} \int_{\eta^m}^{\eta^{m+1}} S\left(\frac{c^0 \eta'}{h}\right) \mathcal{G}_m(\eta') \mathcal{N}(\xi, \eta') (\eta' - \eta'_m + i\eta''_m) d\eta'. \quad (193)$$

If, as is assumed, the spectrum of the incident pulse is slowly varying compared to each Gaussian in the series, we can write

$$J(\xi) \approx \sum_{m=0}^\infty \frac{\sqrt{\pi}}{\eta''_m} \frac{S\left(\frac{c^0 \eta'_m}{h}\right)}{\dot{\mathcal{D}}(\xi, \eta_m)} \int_{\eta^m}^{\eta^{m+1}} \mathcal{G}_m(\eta') \mathcal{N}(\xi, \eta') (\eta' - \eta'_m + i\eta''_m) d\eta'. \quad (194)$$

Due to the concentrated nature of the Gaussians, if the limits of each integral were extended beyond the interval $[\eta^m, \eta^{m+1}]$, the contribution of the extended interval integrals would be negligible, so that we can make the approximation

$$J(\zeta) \approx \sum_{m=0}^{\infty} \frac{\sqrt{\pi}}{\eta_m''} \frac{S(\frac{c^0 \eta_m'}{h})}{\mathcal{D}(\zeta, \eta_m)} [K_1(\zeta) + (-\eta_m' + i\eta_m'')K_2(\zeta)], \quad (195)$$

wherein (see (183))

$$K_1(\zeta) = \int_0^{\infty} \mathcal{G}_m(\eta') e^{-i\eta' T(\zeta)} \eta' d\eta' = \frac{1}{\eta_m'' \sqrt{\pi}} \int_0^{\infty} e^{-i\eta' T(\zeta) - \frac{(\eta' - \eta_m')^2}{(\eta_m'')^2}} \eta' d\eta', \quad (196)$$

$$K_2(\zeta) = \int_0^{\infty} \mathcal{G}_m(\eta') e^{-i\eta' T(\zeta)} d\eta' = \frac{1}{\eta_m'' \sqrt{\pi}} \int_0^{\infty} e^{-i\eta' T(\zeta) - \frac{(\eta' - \eta_m')^2}{(\eta_m'')^2}} d\eta'. \quad (197)$$

We make the change of variables

$$\varpi = \frac{2\eta_m' - i(\eta_m'')^2 T(\zeta)}{2}, \quad \xi = \frac{\eta' - \varpi}{\eta_m''}, \quad (198)$$

wherein we assume that $\eta_m'' \ll \varpi$, and use (Abramowitz & Stegun 1986, p. 302)

$$\int_0^z \exp(-\xi^2) d\xi = \frac{\sqrt{\pi}}{2} \operatorname{erf}(z), \quad \operatorname{erf}(\infty) = 1, \quad (199)$$

(in which erf is the error function, so that $\operatorname{erf}(\frac{\varpi}{\eta_m''}) \sim \operatorname{erf}(\infty) = 1$) to find

$$K_2(\zeta) = \exp \left[-i\eta_m' T(\zeta) - \left(\frac{\eta_m'' T(\zeta)}{2} \right)^2 \right], \quad (200)$$

$$K_1(\zeta) = \left(\eta_m' - i \frac{(\eta_m'')^2 T(\zeta)}{2} \right) K_2(\zeta), \quad (201)$$

so that

$$J(\zeta) \approx \sum_{m=0}^{\infty} \frac{\sqrt{\pi}}{\eta_m''} \frac{S(\frac{c^0 \eta_m'}{h})}{\mathcal{D}(\zeta, \eta_m)} \left[\left(\eta_m' - i \frac{(\eta_m'')^2 T(\zeta)}{2} \right) + (-\eta_m' + i\eta_m'') \right] K_2(\zeta), \quad (202)$$

which approximates to,

$$J(\zeta) \approx i\sqrt{\pi} \sum_{m=0}^{\infty} \frac{S(\frac{c^0 \eta_m'}{h})}{\mathcal{D}(\zeta, \eta_m)} \left(1 - \frac{\eta_m'' T(\zeta)}{2} \right) e^{[-i\eta_m' T(\zeta) - (\frac{\eta_m'' T(\zeta)}{2})^2]}. \quad (203)$$

8.3 Evaluation of J_1^1 , J_2^1 and J_3^1

We had

$$J_j^1(\mathbf{x}_g, t, \zeta) = \Re \int_0^{\infty} \frac{S(\frac{c^0 \eta'}{h})}{\mathcal{D}_j(\zeta, \eta')} e^{-i\eta' T_j(\zeta)} d\eta'; \quad j = 1, 2, 3, \quad (204)$$

where

$$T_1(\zeta) := -\frac{(x_1 - x_1^s)}{h} \zeta - \frac{(x_2^s - h)}{h} \psi(\zeta) + \frac{c^0 t}{h}, \quad (205)$$

$$T_j(\zeta) := -\frac{(x_1 - x_1^s)}{h} \zeta - i \frac{(x_2^s - h)}{h} \theta(\zeta) + \frac{c^0 t}{h}; \quad j = 2, 3. \quad (206)$$

Thus,

$$\begin{aligned} J_1^1(\mathbf{x}_g, t, \zeta) &\approx -\Im \sqrt{\pi} \sum_{m=0}^{\infty} \frac{S(\frac{c^0 \eta_m^{Be}}{h})}{\mathcal{D}_1(\zeta, \eta_m^{Be})} \left(1 - \frac{\eta_m^{Be} T_1(\zeta)}{2} \right) e^{[-i\eta_m^{Be} T_1(\zeta) - (\frac{\eta_m^{Be} T_1(\zeta)}{2})^2]} \\ &\quad - \Im \sqrt{\pi} \sum_{m=0}^{\infty} \frac{S(\frac{c^0 \eta_m^{Bo}}{h})}{\mathcal{D}_1(\zeta, \eta_m^{Bo})} \left(1 - \frac{\eta_m^{Bo} T_1(\zeta)}{2} \right) e^{[-i\eta_m^{Bo} T_1(\zeta) - (\frac{\eta_m^{Bo} T_1(\zeta)}{2})^2]}, \end{aligned} \quad (207)$$

$$\begin{aligned} J_2^1(\mathbf{x}_g, t, \zeta) &\approx -\Im \sqrt{\pi} \sum_{m=0}^{\infty} \frac{S(\frac{c^0 \eta_m^{Le}}{h})}{\mathcal{D}_2(\zeta, \eta_m^{Le})} \left(1 - \frac{\eta_m^{Le} T_2(\zeta)}{2} \right) e^{[-i\eta_m^{Le} T_2(\zeta) - (\frac{\eta_m^{Le} T_2(\zeta)}{2})^2]} \\ &\quad - \Im \sqrt{\pi} \sum_{m=0}^{\infty} \frac{S(\frac{c^0 \eta_m^{Lo}}{h})}{\mathcal{D}_2(\zeta, \eta_m^{Lo})} \left(1 - \frac{\eta_m^{Lo} T_2(\zeta)}{2} \right) e^{[-i\eta_m^{Lo} T_2(\zeta) - (\frac{\eta_m^{Lo} T_2(\zeta)}{2})^2]}, \end{aligned} \quad (208)$$

$$\begin{aligned}
 J_3^1(\mathbf{x}_g, t, \zeta) \approx & -\Im \sqrt{\pi} \sum_{m=0}^{\infty} \frac{S\left(\frac{c^0 \eta_m^{Se}}{h}\right)}{\mathcal{D}_3(\zeta, \eta_m^{Se})} \left(1 - \frac{\eta_m^{Se} T_3(\zeta)}{2}\right) e^{[-i \eta_m^{Se} T_3(\zeta) - (\frac{\eta_m^{Se} T_3(\zeta)}{2})^2]} \\
 & - \Im \sqrt{\pi} \sum_{m=0}^{\infty} \frac{S\left(\frac{c^0 \eta_m^{So}}{h}\right)}{\mathcal{D}_3(\zeta, \eta_m^{So})} \left(1 - \frac{\eta_m^{So} T_3(\zeta)}{2}\right) e^{[-i \eta_m^{So} T_3(\zeta) - (\frac{\eta_m^{So} T_3(\zeta)}{2})^2]}.
 \end{aligned} \tag{209}$$

8.3.1 Contribution of u_1^1 to the time-domain ground displacement

On account of (143) and (147) we have

$$\begin{aligned}
 u_1^1(\mathbf{x}_g, t) = & \Im \sum_{m=0}^{\infty} S\left(\frac{c^0 \eta_m^{Be}}{h}\right) \int_{-1}^1 \mathcal{P}_m^{Be}(\mathbf{x}_g, \mathbf{x}^s, \zeta) e^{-i \eta_m^{Be} (U_1(\mathbf{x}_g, \mathbf{x}^s, \zeta) + \frac{c^0}{h} t)} \\
 & \times e^{-[U_1^2(\mathbf{x}_g, \mathbf{x}^s, \zeta) + 2U_1(\mathbf{x}_g, \mathbf{x}^s, \zeta) \frac{c^0}{h} t + (\frac{c^0}{h} t)^2] \frac{\eta_m^{Be 2}}{4}} \\
 & + \Im \sum_{m=0}^{\infty} S\left(\frac{c^0 \eta_m^{Bo}}{h}\right) \int_{-1}^1 \mathcal{P}_m^{Bo}(\mathbf{x}_g, \mathbf{x}^s, \zeta) e^{-i \eta_m^{Bo} (U_1(\mathbf{x}_g, \mathbf{x}^s, \zeta) + \frac{c^0}{h} t)} \\
 & \times e^{-[U_1^2(\mathbf{x}_g, \mathbf{x}^s, \zeta) + 2U_1(\mathbf{x}_g, \mathbf{x}^s, \zeta) \frac{c^0}{h} t + (\frac{c^0}{h} t)^2] \frac{\eta_m^{Bo 2}}{4}},
 \end{aligned} \tag{210}$$

wherein

$$\mathcal{P}_m^{Be}(\mathbf{x}_g, \mathbf{x}^s, \zeta) := \frac{c^0}{h \sqrt{\pi}} \frac{\left(1 - \frac{\eta_m^{Be}}{2} (U_1(\mathbf{x}_g, \mathbf{x}^s, \zeta) + \frac{c^0}{h} t)\right)}{\mathcal{D}_1(\zeta, \eta_m^{Be})}, \tag{211}$$

$$\mathcal{P}_m^{Bo}(\mathbf{x}_g, \mathbf{x}^s, \zeta) := \frac{c^0}{h \sqrt{\pi}} \frac{\left(1 - \frac{\eta_m^{Bo}}{2} (U_1(\mathbf{x}_g, \mathbf{x}^s, \zeta) + \frac{c^0}{h} t)\right)}{\mathcal{D}_1(\zeta, \eta_m^{Bo})}, \tag{212}$$

$$U_1(\mathbf{x}_g, \mathbf{x}^s, \zeta) = -X_1 \zeta - X_2 \psi(\zeta), \tag{213}$$

$$X_1 = \frac{x_1 - x_1^s}{h}, \quad X_2 = \frac{x_2^s - h}{h}. \tag{214}$$

More explicitly:

$$\begin{aligned}
 u_1^1(\mathbf{x}_g, t) = & \Im \sum_{m=0}^{\infty} S\left(\frac{c^0 \eta_m^{Be}}{h}\right) \int_{-1}^1 \mathcal{P}_m^{Be}(\mathbf{x}_g, \mathbf{x}^s, \zeta) e^{i[X_1 \zeta + X_2 \psi(\zeta) - \frac{c^0}{h} t] \eta_m^{Be}} \\
 & \times e^{-[X_1^2 \zeta^2 + X_2^2 \psi^2(\zeta) + (\frac{c^0}{h} t)^2 + 2X_1 X_2 \zeta \psi(\zeta) - 2(X_1 \zeta + X_2 \psi(\zeta)) \frac{c^0}{h} t] \frac{\eta_m^{Be 2}}{4}} d\zeta \\
 & + \Im \sum_{m=0}^{\infty} S\left(\frac{c^0 \eta_m^{Bo}}{h}\right) \int_{-1}^1 \mathcal{P}_m^{Bo}(\mathbf{x}_g, \mathbf{x}^s, \zeta) e^{i[X_1 \zeta + X_2 \psi(\zeta) - \frac{c^0}{h} t] \eta_m^{Bo}} \\
 & \times e^{-[X_1^2 \zeta^2 + X_2^2 \psi^2(\zeta) + (\frac{c^0}{h} t)^2 + 2X_1 X_2 \zeta \psi(\zeta) - 2(X_1 \zeta + X_2 \psi(\zeta)) \frac{c^0}{h} t] \frac{\eta_m^{Bo 2}}{4}} d\zeta.
 \end{aligned} \tag{215}$$

Remark 1 $u_1^1(\mathbf{x}_g, t)$ is the time history corresponding to the frequency domain response function $I_1^1(\mathbf{x}_g, \omega)$, which was shown previously to take the form of an integral over the variable ζ (or, equivalently, over the horizontal wavenumber k_1), of type 1 standing body waves (SBW1) (modified somewhat when the layer is dissipative). Here, the same type of integral makes its appearance, but the integrand involves a generic wavefunction of the form

$$\mathcal{U}_{1m}^1(\mathbf{x}_g, t, \zeta) := \Im \mathcal{Q}_{1m}(X_1, X_2, t, \zeta) e^{i[X_1 \zeta + X_2 \psi(\zeta) - \frac{c^0}{h} t] \eta_m^B}, \tag{216}$$

wherein the amplitude function is

$$\begin{aligned}
 \mathcal{Q}_{1m}(X_1, X_2, t, \zeta) := & \mathcal{P}_m^B(\mathbf{x}_g, \mathbf{x}^s, \zeta) \\
 & \times e^{-[X_1^2 \zeta^2 + X_2^2 \psi^2(\zeta) + (\frac{c^0}{h} t)^2 + 2X_1 X_2 \zeta \psi(\zeta) - 2(X_1 \zeta + X_2 \psi(\zeta)) \frac{c^0}{h} t] \frac{\eta_m^B 2}{4}}.
 \end{aligned} \tag{217}$$

Since η_m^B is real, the factor $e^{i[X_1 \zeta + X_2 \psi(\zeta) - \frac{c^0}{h} t] \eta_m^B}$ represents a sinusoidal function of space and time, and since the argument of $e^{-[X_1^2 \zeta^2 + X_2^2 \psi^2(\zeta) + (\frac{c^0}{h} t)^2 + 2X_1 X_2 \zeta \psi(\zeta) - 2(X_1 \zeta + X_2 \psi(\zeta)) \frac{c^0}{h} t] \frac{\eta_m^B 2}{4}}$ is positive for large enough t , it is correct to say that the generic waveform $\mathcal{U}_{1m}^1(\mathbf{x}_g, t, \zeta)$ is an exponentially attenuated sinusoid as a function of the temporal variable t for large-enough t .

Remark 2 The attenuation rate can vary from being a linear function of t for small t to a quadratic function of t for large t , and both of these functions depend on the vertical distance of the source from the lower boundary of the layer, as well as on the epicentral distance (through the functions X_1 and X_2).

Remark 3 The term $e^{-X_2^2 \psi^2 \frac{(\eta_m^B)^2}{4}}$ is generally small (and therefore, the attenuation is large) due to the fact that $(\eta_m^B)^2$ is small; the only situation in which this term can possibly be $\mathcal{O}(1)$ is for large X_2 , which occurs when the focal depth is large, or more precisely, when the vertical distance between the the source and the lower boundary of the layer is much greater than the layer thickness. This means that the $\mathcal{U}_{1m}^1(\mathbf{x}_g, t, \zeta)$ generally contributes significantly to the overall time history only if the the source is relatively deep and/or if $\mathcal{P}_m^B(\mathbf{x}_g, \mathbf{x}^s, \zeta)$ is large for some reason (there is some indication that this might be the case for large contrast of densities and/or body wave velocities between the layer and substratum). This indication is in agreement with what was found concerning the SBW1.

Remark 4 $U_{1m}^1(\mathbf{x}_g, t, \zeta)$ is the time history corresponding to the m th order Haskell ‘mode’ with reduced horizontal wavenumber ζ . The total SBW1 time history $u_1^1(\mathbf{x}_g, t, \zeta)$ represents a sum over all these (even and odd) Haskell ‘mode’ time histories. If, as is often the case, the spectrum of the source pulse $S(\omega)$ is such as to be significant only for low frequencies, only the $m = 0$ *Bo* mode contributes to a great extent to $u_1^1(\mathbf{x}_g, t, \zeta)$.

8.3.2 Contribution of u_2^1 to the time-domain ground displacement

On account of (143) and (208) we have

$$\begin{aligned} u_2^1(\mathbf{x}_g, t) &= \Im \sum_{m=0}^{\infty} S \left(\frac{c^0 \eta_m^{Le}}{h} \right) \left\{ \int_{-\Re\gamma}^{-1} + \int_1^{\Re\gamma} \right\} \mathcal{P}_m^{Le}(\mathbf{x}_g, \mathbf{x}^s, \zeta) e^{-i\eta_m^{Le}(U_2(\mathbf{x}_g, \mathbf{x}^s, \zeta) + \frac{c^0}{h}t)} \\ &\quad \times e^{-(U_2^2(\mathbf{x}_g, \mathbf{x}^s, \zeta) + 2U_2(\mathbf{x}_g, \mathbf{x}^s, \zeta)\frac{c^0}{h}t + (\frac{c^0}{h}t)^2)\frac{(\eta_m^{Le})^2}{4}} \\ &+ \Im \sum_{m=0}^{\infty} S \left(\frac{c^0 \eta_m^{Lo}}{h} \right) \left\{ \int_{-\Re\gamma}^{-1} + \int_1^{\Re\gamma} \right\} \mathcal{P}_m^{Lo}(\mathbf{x}_g, \mathbf{x}^s, \zeta) e^{-i\eta_m^{Lo}(U_2(\mathbf{x}_g, \mathbf{x}^s, \zeta) + \frac{c^0}{h}t)} \\ &\quad \times e^{-(U_2^2(\mathbf{x}_g, \mathbf{x}^s, \zeta) + 2U_2(\mathbf{x}_g, \mathbf{x}^s, \zeta)\frac{c^0}{h}t + (\frac{c^0}{h}t)^2)\frac{(\eta_m^{Lo})^2}{4}}, \end{aligned} \quad (218)$$

wherein

$$\mathcal{P}_m^{Le}(\mathbf{x}_g, \mathbf{x}^s, \zeta) := \frac{c^0}{h\sqrt{\pi}} \frac{(1 - \frac{\eta_m^{Le}}{2}(U_2(\mathbf{x}_g, \mathbf{x}^s, \zeta) + \frac{c^0}{h}t))}{\tilde{D}_2(\zeta, \eta_m^{Le})}, \quad (219)$$

$$\mathcal{P}_m^{Lo}(\mathbf{x}_g, \mathbf{x}^s, \zeta) := \frac{c^0}{h\sqrt{\pi}} \frac{(1 - \frac{\eta_m^{Lo}}{2}(U_2(\mathbf{x}_g, \mathbf{x}^s, \zeta) + \frac{c^0}{h}t))}{\tilde{D}_2(\zeta, \eta_m^{Lo})}, \quad (220)$$

$$U_2(\mathbf{x}_g, \mathbf{x}^s, \zeta) = -X_1\zeta - iX_2\theta(\zeta). \quad (221)$$

More explicitly:

$$\begin{aligned} u_2^1(\mathbf{x}_g, t) &= \Im \sum_{m=0}^{\infty} S \left(\frac{c^0 \eta_m^{Le}}{h} \right) \left\{ \int_{-\Re\gamma}^{-1} + \int_1^{\Re\gamma} \right\} \mathcal{P}_m^{Le}(\mathbf{x}_g, \mathbf{x}^s, \zeta) \\ &\quad \times e^{i[(X_1\zeta - \frac{c^0}{h}t)\eta_m^{Le} + X_2\theta(\zeta)(\frac{c^0}{h}t - X_1\zeta)\frac{(\eta_m^{Le})^2}{2}]} \\ &\quad \times e^{-[X_2\theta(\zeta)\eta_m^{Le} + (X_1^2\zeta^2 - X_2^2\theta^2(\zeta) + (\frac{c^0}{h}t)^2 - 2X_1\zeta\frac{c^0}{h}t)\frac{(\eta_m^{Le})^2}{4}]} d\zeta \\ &+ \Im \sum_{m=0}^{\infty} S \left(\frac{c^0 \eta_m^{Lo}}{h} \right) \left\{ \int_{-\Re\gamma}^{-1} + \int_1^{\Re\gamma} \right\} \mathcal{P}_m^{Lo}(\mathbf{x}_g, \mathbf{x}^s, \zeta) \\ &\quad \times e^{i[(X_1\zeta - \frac{c^0}{h}t)\eta_m^{Lo} + X_2\theta(\zeta)(\frac{c^0}{h}t - X_1\zeta)\frac{(\eta_m^{Lo})^2}{2}]} \\ &\quad \times e^{-[X_2\theta(\zeta)\eta_m^{Lo} + (X_1^2\zeta^2 - X_2^2\theta^2(\zeta) + (\frac{c^0}{h}t)^2 - 2X_1\zeta\frac{c^0}{h}t)\frac{(\eta_m^{Lo})^2}{4}]} d\zeta. \end{aligned} \quad (222)$$

Remark 1 $u_2^1(\mathbf{x}_g, t)$ is the time history corresponding to the frequency domain response function $I_2^1(\mathbf{x}_g, \omega)$, which was shown previously to take the form of an integral over the variable ζ (or, equivalently, over the horizontal wavenumber k_1), of type 2 standing body waves (SBW2) (modified somewhat when the layer is dissipative). Here, the same type of integral makes its appearance, but the integrand involves a generic wavefunction of the form

$$\mathcal{U}_{2m}^1(\mathbf{x}_g, t, \zeta) := \Im \mathcal{Q}_{2m}(X_1, X_2, t, \zeta) e^{i[(X_1\zeta - \frac{c^0}{h}t)\eta_m^{Le} + X_2\theta(\zeta)(\frac{c^0}{h}t - 2X_1\zeta)\frac{(\eta_m^{Le})^4}{4}]} \eta_m^{Le}, \quad (223)$$

wherein the amplitude function is

$$\mathcal{Q}_{2m}(X_1, X_2, t, \zeta) := \mathcal{P}_m^L(\mathbf{x}_g, \mathbf{x}^s, \zeta) \times e^{-[X_2\theta(\zeta)\eta_m^{\prime L} + (X_1^2\zeta^2 - X_2^2\theta^2(\zeta) + (\frac{c_0}{h}t)^2 - 2X_1\zeta\frac{c_0}{h}t)\frac{(\eta_m^{\prime L})^2}{4} - 1]}. \quad (224)$$

Since $\eta_m^{\prime L}$ is real, and $|\eta_m^{\prime L}| \gg |\eta_m^{\prime\prime L}|$, the factor $e^{iL\eta_m^{\prime L}} \sim e^{iL(X_1\zeta - \frac{c_0}{h}t)\eta_m^{\prime L}}$ in (223) represents a sinusoidal function of space and time, and since the argument of e^{-1} in (224) is positive for large enough t , it is correct to say that the generic waveform $\mathcal{U}_{2m}^L(\mathbf{x}_g, t, \zeta)$ is an exponentially-attenuated sinusoid as a function of the temporal variable t for large-enough t .

Remark 2 The attenuation rate can vary from being a constant with respect to t for small t to a quadratic function of t for large t ; only the small- t function depends significantly on the vertical distance of the source from the lower boundary of the layer and (to a lesser extent) on the epicentral distance, whereas the large- t function does not depend significantly either on the focal depth or on the epicentral distance.

Remark 3 The term $e^{-X_2\theta\eta_m^{\prime L}}$ in \mathcal{Q}_{2m} is generally small (and therefore the attenuation is large) due to the fact that $\eta_m^{\prime L}$ is positive and relatively large; the only situation in which this term can possibly be $\mathcal{O}(1)$ is for small X_2 , which occurs when the focal depth is small, or more precisely, when the vertical distance between the source and the lower boundary of the layer is much smaller than the layer thickness. This means that $\mathcal{U}_{2m}^L(\mathbf{x}_g, t, \zeta)$ contributes all the more significantly to the overall time history the closer the source is, in the vertical direction, to the lower boundary of the layer, and/or if $\mathcal{P}_m^L(\mathbf{x}_g, \mathbf{x}^s, \zeta)$ is large for some reason. This indication is in agreement with what was found concerning the SBW2.

Remark 4 $U_{2m}^1(\mathbf{x}_g, t, \zeta)$ is the time history corresponding to the m -th order Love mode with reduced horizontal wavenumber ζ . The total SBW2 time history $u_2^1(\mathbf{x}_g, t, \zeta)$ represents a sum over all these (even and odd) Love mode time histories. If, as is often the case, the spectrum of the source pulse $S(\omega)$ is such as to be significant only for low frequencies, only the $m = 0$ *Lo* mode contributes to a great extent to $u_2^1(\mathbf{x}_g, t, \zeta)$.

8.3.3 Contribution of u_3^1 to the time-domain ground displacement

On account of the remarks at the end of Section 5.5 the contribution of u_3^1 to the time-domain ground displacement can be considered to be negligible.

8.4 Characteristics of the time history of total ground response

The material in the previous three sections suggests that the time domain response takes the form:

$$u^1(\mathbf{x}_g, t) \approx \Im \sum_{l=1}^L S(\omega_l) H(\mathbf{x}_g, \mathbf{x}^s, \omega_l) e^{-\frac{\mathcal{F}(\mathbf{x}_g, \mathbf{x}^s, \omega_l)}{f(\mathbf{x}_g, \mathbf{x}^s, \omega_l)} t} e^{i[\varpi(\mathbf{x}_g, \mathbf{x}^s, \omega_l)t + \zeta(\mathbf{x}_g, \mathbf{x}^s, \omega_l)]}, \quad (225)$$

or, with the notations $S_l = S(\omega_l)$, $H_l = H(\mathbf{x}_g, \mathbf{x}^s, \omega_l)$, $\mathcal{F}_l = \mathcal{F}(\mathbf{x}_g, \mathbf{x}^s, \omega_l)$, $f_l = f(\mathbf{x}_g, \mathbf{x}^s, \omega_l)$, $\varpi_l = \varpi(\mathbf{x}_g, \mathbf{x}^s, \omega_l)$, $\zeta_l = \zeta(\mathbf{x}_g, \mathbf{x}^s, \omega_l)$,

$$u^1(\mathbf{x}_g, t) \approx \Im \sum_{l=1}^L S_l H_l e^{-\frac{\mathcal{F}_l}{f_l} t} e^{i[\varpi_l t + \zeta_l]}, \quad (226)$$

wherein L is a positive integer, ω_l is a resonance (i.e. of a Love mode) or pseudo-resonance (of a Haskell ‘mode’) frequency, S_l the source spectrum function at angular frequency ω_l , H_l an amplitude function at angular frequency ω_l , \mathcal{F}_l an attenuation function at angular frequency ω_l , f_l the sharpness of a resonance or pseudo-resonance peak at angular frequency ω_l , ϖ_l the angular frequency of the sinusoidal variation of the contribution of the resonance or pseudo resonance term at angular frequency ω_l , and ζ_l the phase of the sinusoidal variation of the contribution of the resonance or pseudo resonance term at angular frequency ω_l . Note that the sharpness is 1/width at half-height of a frequency-domain resonance or pseudo-resonance peak, so that the sharpness is all the larger the more the peak resembles a Dirac delta distribution.

Using the complex representations of S_l and H_l :

$$S_l = \|S_l\| e^{i\sigma_l}, \quad H_l = \|H_l\| e^{i\tau_l}, \quad (227)$$

and the designations

$$C_l := \|S_l\| \|H_l\|, \quad \xi_l := \zeta_l + \sigma_l + \tau_l, \quad (228)$$

we get

$$u^1(\mathbf{x}_g, t) \approx \Im \sum_{l=1}^L C_l e^{-\frac{\mathcal{F}_l}{f_l} t} e^{i(\varpi_l t + \xi_l)}. \quad (229)$$

Consider the case $L = 1$. Then

$$u^1(\mathbf{x}_g, t) \approx C_1 e^{-\frac{\mathcal{F}_1}{f_1} t} \sin(\varpi_1 t + \xi_1). \quad (230)$$

which simply represents a time-attenuated sinusoidal function of time. The frequency of the sinusoid is ϖ_1 and the attenuation rate is inversely proportional to the sharpness f_1 which means that the smaller is the sharpness, the shorter is the duration of ground response signal. We shall see in the companion paper (Groby & Wirgin 2005) that (relatively) short-duration time-domain response is typically obtained for deep sources whose spectrum is such as to give a dominant contribution from the fundamental Haskell pseudo-resonance. This response is similar

to what one obtains with the 1-D analysis and obviously cannot account for the long-duration signals with beating that has frequently been observed in urban sites such as Mexico City.

Let us next consider the case $L = 2$. Then it is easy to show that:

$$u^1(\mathbf{x}_g, t) \approx \left(C_2 e^{-\frac{\mathcal{F}_2}{T_2} t} + C_1 e^{-\frac{\mathcal{F}_1}{T_1} t} \right) \sin(\varpi_+ t + \xi_+) \cos(\varpi_- t + \xi_-) \\ + \left(C_2 e^{-\frac{\mathcal{F}_2}{T_2} t} - C_1 e^{-\frac{\mathcal{F}_1}{T_1} t} \right) \sin(\varpi_- t + \xi_-) \cos(\varpi_+ t + \xi_+), \quad (231)$$

which represents a combination of two amplitude-modulated time-attenuated sinusoidal signals with carrier angular frequencies $\varpi_+ = \frac{\varpi_2 + \varpi_1}{2}$. Note that $\xi_{\pm} = \frac{\xi_2 \pm \xi_1}{2}$, $\varpi_- = \frac{\varpi_2 - \varpi_1}{2}$, and that the period of the modulation $|\frac{2\pi}{\varpi_-}|$ is larger than that of the carrier signals $\frac{2\pi}{\varpi_+}$.

Remark 1 Eq. (231) generally describes a time-attenuated carrier (sinusoidal) signal exhibiting irregular beating effects (due to the sinusoidal modulation functions).

Remark 2 If the carrier frequency is close to the fundamental Love mode resonance and fundamental Haskell pseudo-mode resonance frequencies (both of these having been shown previously to be close to each other), then we can conclude that the response is dominated by coupling to the fundamental Love mode and Haskell pseudo-mode.

Remark 3 If, on the other hand, the carrier frequency is much larger than either the fundamental Love mode resonance and fundamental Haskell pseudo-mode resonance frequencies, then we can conclude that the response is dominated by coupling to either the fundamental Love mode and first-order Haskell pseudo-mode, or to the fundamental Haskell pseudo-mode and first-order Love mode (under the assumption that the fundamental and first-order resonances and pseudo-resonances are dominant in the spectra).

Remark 4 An interesting, although perhaps academic, situation arises when $C_2 e^{-\frac{\mathcal{F}_2}{T_2} t} \approx C_1 e^{-\frac{\mathcal{F}_1}{T_1} t}$, in which case we obtain

$$u^1(\mathbf{x}_g, t) \approx 2C_1 e^{-\frac{\mathcal{F}_1}{T_1} t} \sin(\varpi_+ t + \xi_+) \cos(\varpi_- t + \xi_-), \quad (232)$$

which represents a pure time-attenuated sinusoidal carrier signal of angular frequency ϖ_+ , amplitude-modulated by a pure cosinusoidal function of angular frequency ϖ_- . We shall see in the companion paper (Groby & Wirgin 2005) that such ground response time histories can actually be found to occur, and that they are due essentially to coupling to the fundamental Love mode and Haskell pseudo-mode due to the fact that the carrier frequency of the modulated signal is close to the resonance frequencies of this mode and pseudo-mode.

9 DISCUSSION

We shall now attempt to provide answers to the questions raised in Section 1. These are completed in the companion paper.

The *first question* was: is it possible to obtain anomalous response without any lateral heterogeneity in the underground medium?

The configuration studied herein was *laterally homogeneous*. We have shown that the 1-D response only accounts for interference effects (as embodied by the SBW1), but not for coupling to Love modes (as embodied by the SBW2) in the layer, which is particularly strong when the source is in the neighborhood of the lower boundary of the layer.

Insofar as anomalous effects are essentially characterized by long duration and beating phenomena in the signals, the answer to this question is negative as concerns the 1-D response. However, when the contrast of material properties between the layer and substratum is very large, it is possible to obtain fairly long duration signals (albeit without beating), which are essentially associated with the 1-D response, even when the source is far from the lower boundary of the layer.

More generally, that is, when coupling to Love modes is achieved, the answer to the question is positive.

The *second question* was: what is the relation of the 1-D to the 2-D response and how adequate is it to model the general response of the configuration by its response to a (nearly) vertically incident plane wave?

We have shown that not only does the 1-D model not give rise to resonance phenomena, but that truly resonant phenomena associated with the excitation of Love modes can only be described by a fully 2-D (or 3-D) model.

For a source deep below the lower boundary of the layer, the response is essentially due to the contributions of the SBW1 (more or less equivalent to the 1-D response), but when the depth of the source is close to that of the lower boundary of the layer the waves (SBW2) not included in the 1-D model play a major role in the overall response in that they either overwhelm the 1-D response (long duration response without beating) or combine with the 1-D response to produce signals with long duration and beating, which facts were revealed in explicit manner by the direct time-domain analysis in Section 8. These findings should be taken into account in relation to studies (e.g. Sandi *et al.* 2004) that attempt to predict seismic response of urban sites from 1-D type of analysis.

The *third question* was: how does the focal depth of the source affect the response? The answer to this question is provided in the previous two paragraphs. However, it is opportune to reconsider this question in the light of topic (b) concerning the effects of underlying soil heterogeneities, lateral variations of the underlying soil layer, and built environment on seismic response in urban sites. One can show (Wirgin 2002) that a wave incident on a heterogeneous medium gives rise to a diffracted wave which can be considered to be radiated by *induced sources* (as opposed to the *active source* associated with the primary seismic disturbance) located within the medium. These induced sources can also appear on the boundary of the medium (especially at endpoints, corners and irregularities of the boundary), so that the edges of a soft basin or the stress-free ground which includes the buildings overlying a homogeneous soft layer in a city-like site, can also constitute the locations of intense induced sources in response to an incident seismic wave. The fields radiated by all these induced sources can be

represented in a manner similar (provided the basic geometry of the configuration is similar) to that of the present work, so that much of what was written and found above, notably concerning the response to active sources located outside, and in the vicinity of the soft layer (and, by extension, to induced sources located *within or on the boundaries of* the soft layer), should apply to city-like sites built on soft layers or basins.

The most important point (mentioned in references such as Tsogka & Wirgin (2003), implicit in Igel *et al.* (2002), Jahnke *et al.* (2002), and proven herein as concerns active sources) is the following: the presence of these active or induced sources, located *near or within* the soft layer overlying a relatively hard substratum, enables coupling to Love-type modes which may be responsible for a part of the anomalous ground response observed in cities such as Mexico, notably motion characterized by long durations and beatings.

Naturally, the above remarks apply only to the 2-D SH polarization case studied herein; it will be interesting to find out if they carry over to the 2-D *P-SV* case, with Rayleigh–Lamb modes playing the role of the Love modes described above. Scattering may, of course, add to the duration-lengthening effects, insofar as it can be attributed to radiation by induced sources, but this question will probably require more sophisticated theoretical models and confirmation via numerical studies (as is done in publications such as Furumura & Kennett 1998).

The answers to the fourth, fifth, sixth and seventh questions are provided in the companion paper (Groby & Wirgin 2005) wherein concluding comments will be given for the contents of the two papers.

ACKNOWLEDGMENTS

This research was carried out partially within the framework of the Action Concertée Incitative ‘Prévention des Catastrophes Naturelles’ entitled ‘Interaction ‘site-ville’ et aléa sismique en milieu urbain’ of the French Ministry of Research.

REFERENCES

- Abramowitz, M. & Stegun, A., 1986. *Handbook of Mathematical Functions*, Dover, New York.
- Apsel, R.J. & Luco, J.E., 1983. On the Green’s function for a layered half-space. Part II, *Bull. seism. Soc. Am.*, **73**, 931–951.
- Attwood, S.S., 1951. Surface wave propagation over a coated plane conductor, *J. Appl. Phys.*, **22**, 504–509.
- Balendra, T. & Kong, K.H., 2004. Effects of ground motions in Singapore due to far-field earthquakes, *Proc. 11th International Conference on Soil Dynamics & Earthquake Engineering*, 255–259.
- Bard, P.-Y., 1985. Les effets de site d’origine structurale: principaux résultats expérimentaux et théoriques, in *Génie Parasismique*, pp. 223–238, ed. Davidovici, V., Presses de l’Ecole Nationale des Ponts et Chaussées, Paris.
- Bard, P.-Y. & Bouchon, M., 1980. The seismic response of sediment-filled valleys. part I. The case of incident SH waves, *Bull. seism. Soc. Am.*, **70**, 1263–1286.
- Bard, P.-Y. & Bouchon, M., 1985. The two-dimensional resonance of sediment-filled valleys, *Bull. seism. Soc. Am.*, **75**, 519–541.
- Bard, P.-Y., Eeri, M., Campillo, M., Chávez-García, F.J. & Sanchez-Sesma, F.J., 1988. The Mexico earthquake of September 19, 1985—a theoretical investigation of large- and small-scale amplification effects in the Mexico City valley, *Earthquake Spectra*, **4**, 609–633.
- Ben-Menahem, A. & Harkrider, D.G., 1964. Radiation patterns of seismic waves from buried dipolar point sources in a flat stratified earth, *J. geophys. Res.*, **69**, 2605–2620.
- Ben-Zion, Y. & Aki, K., 1990. Seismic radiation from a SH line source in a laterally heterogeneous planar fault zone, *Bull. seism. Soc. Am.*, **90**, 971–994.
- Boore, D.M., 2003. Can site response be predicted? *J. Earthquake Engrg.*, submitted.
- Bouchon, M., 1982. The complete synthesis of seismic crustal phases at regional distance, *J. geophys. Res.*, **87**(B3) 1735–1741.
- Boutin, C. & Roussillon, P., 2004. Assessment of the urbanization effect on seismic response, *Bull. seism. Soc. Am.*, **94**, 251–268.
- Campillo, M., Gariel, J.C., Aki, K. & Sanchez-Sesma F.J., 1989. Destructive ground motion in Mexico City: source, path, and site effects during great 1985 Michoacan earthquake, *Bull. seism. Soc. Am.*, **79**, 1718–1735.
- Cárdenas, M. & Chávez-García, F.J., 2003. Regional path effects on seismic wave propagation in central Mexico, *Bull. seism. Soc. Am.*, **93**, 973–985.
- Carrier, G.F., Krook, M. & Pearson, C.E., 1983. *Functions of a Complex Variable*, Hod Books, Ithaca.
- Celebi, M., 2004. Responses of a 14-story (Anchorage, AK) building to far-distance ($M_s = 7.9$) Denali (2002) and near distance earthquakes in 2002, *Proc. 11th International Conference on Soil Dynamics & Earthquake Engineering*, pp. 895–900, eds Doolin, D. *et al.*, Stallion Press, Berkeley.
- Chávez-García, F.J. & Bard, P.-Y., 1994. Site effects in Mexico City eight years after the September 1985 Michoacan earthquakes, *Soil Dyn. Earthquake Engrg.*, **13**, 229–247.
- Chávez-García, F.J., Ramos-Martínez, J. & Romero-Jiménez, E., 1995. Surface-wave dispersion analysis in Mexico City, *Bull. seism. Soc. Am.*, **85**, 1116–1126.
- Chen, C.-H., Teng, T.-L. & Gung, Y.-C., 1998. Ten-second Love-wave propagation and strong ground motions in Taiwan, *J. geophys. Res.*, **103**(B9), 21 253–21 273.
- Collins, R.E., 1960. *Field Theory of Guided Waves*, Chapter 11, Mc Graw-Hill, New York.
- Dravinski, M. & Mossessian, T.K., 1988. On evaluation of the Green function for harmonic line loads in an elastic half-space, *J. Num. Meth. Engrg.*, **26**, 823–841.
- Ewing, M., Jardetzky, W.S. & Press, F., 1957. *Elastic Waves in Layered Media*, McGraw Hill, New York.
- Faeh, D. & Panza, G.F., 1994. Realistic modeling of observed seismic motion in complex sedimentary basins, *Annal. Geofis.*, **37**, 1771–1797.
- Faeh, D., Suhadolc, P., Mueller, S. & Panza, G.F., 1994. A hybrid method for the estimation of ground motion in sedimentary basins: quantitative modeling of Mexico City, *Bull. seism. Soc. Am.*, **84**, 383–399.
- Furumura, T. & Kennett, B.L.N., 1998. On the nature of regional seismic phases-III. The influence of crustal heterogeneity on the wavefield for subduction earthquakes: the 1985 Michoacan and 1995 Copala, Guerrero, Mexico earthquakes, *Geophys. J. Int.*, **135**, 1060–1084.
- Groby, J.-P., Tsogka, C. & Wirgin, A., 2004. A time domain method for modeling viscoelastic SH wave propagation in a city-like environment, *Proc. 11th International Conference on Soil Dynamics & Earthquake Engineering*, pp. 887–894, eds Doolin, D. *et al.*, Stallion Press, Berkeley.
- Groby, J.-P. & Wirgin, A., 2005. 2-D ground motion at a soft viscoelastic layer/hard substratum site in response to SH cylindrical seismic waves radiated by deep and shallow line sources — II. Numerical results, *Geophys. J. Int.*, doi:10.1111/j.1365-246X.2005.02713.x.
- Harkrider, D.G., 1964. Surface waves in multilayered elastic media. part I: Rayleigh and Love waves from buried sources in a multilayered elastic half-space, *Bull. seism. Soc. Am.*, **54**, 627–679.
- Harkrider, D.G., 1970. Surface waves in multilayered elastic media. part II: higher mode spectra and spectral ratios from point sources in plane layered earth models, *Bull. seism. Soc. Am.*, **60**, 1937–1987.
- Hisada, Y., Yamamoto, S. & Tani S., 1988. Analysis of strong ground motion of plain and basin being composed of soft soil by fault model and boundary element method, in *Proc. Ninth World Conference on*

- Earthquake Engineering*, Paper 88, Japan Association for Earthquake Disaster Prevention, Tokyo.
- Igel, H., Jahnke, G. & Ben-Zion, Y., 2002. Numerical simulation of fault zone guided waves: accuracy and 3-D effects, *Pure appl. Geophys.*, **159**, 2067–2083.
- Jahnke, G., Igel, H. & Ben-Zion, Y., 2002. Three-dimensional calculations of fault-zone-guided waves in various irregular structures, *Geophys. J. Int.*, **151**, 416–426.
- Kanamori, H. & Given, J.W., 1981. Use of long-period surface waves for rapid determination of earthquake-source parameters, *Phys. Earth planet. Int.*, **27**, 8–31.
- Kennett, B.L.N., 1983. *Seismic Wave Propagation in Stratified Media*, Cambridge University Press, Cambridge.
- Kjartansson, E., 1979. Constant Q wave propagation and attenuation, *J. geophys. Res.*, **84**, 4737–4748.
- Lee, D.M., Jennings, P.C. & Housner, G.W., 1980. A selection of important strong motion earthquake records, *Technical Rept. California Institute of Technology*, EERL-80-01.
- Ling, R.T., Scholler, J.D. & Ufimtsev P.Y., 1998. The propagation and excitation of surface waves in an absorbing layer, *Prog. Electromag. Res.*, **19**, 49–91.
- Luco, J.E. & Apsel, R.J., 1983. On the Green's function for a layered half-space. part I, *Bull. seism. Soc. Am.*, **73**, 909–929.
- Mendiguren, J.A., 1977. Inversion of surface wave data in source mechanism studies, *J. geophys. Res.*, **82**, 889–894.
- Morse, P.M. & Feshbach, H., 1953. *Methods of Theoretical Physics*, McGraw Hill, New York.
- Novikova, E.I. & Trifunac, M.D., 1993. Duration of strong earthquake ground motion: physical basis and empirical equations, *Technical Rept. University of Southern California, Dept. Civil Engineering*, CE 93-02.
- Novikova, E.I. & Trifunac, M.D., 1995. Frequency dependent duration of strong earthquake ground motion: updated empirical equations, *Technical Rept. University of Southern California, Dept. Civil Engineering*, CE 95-01.
- Panza, G.F., 1981. The resolving power of seismic surface wave with respect to crust and upper mantle structural models, in *The Solution of the Inverse Problem in Geophysical Interpretation*, pp. 39–77, ed. Cassinis, R., Plenum, New York.
- Panza, G.F., 1985. Synthetic seismograms: the Rayleigh waves modal summation, *J. Geophys.*, **58**, 125–145.
- Panza, G.F., Romanelli, F. & Vaccari, F., 2000a. Realistic modelling of waveforms in laterally heterogeneous anelastic media by modal summation, *Geophys. J. Int.*, **143**, 340–352.
- Panza, G.F., Romanelli, F. & Vaccari, F., 2000b. Seismic wave propagation in laterally heterogeneous anelastic media: theory and applications to the seismic zonation, *Advances in Geophysics*, pp. 1–95, eds Doolin, D., Kammerer, A., Nogami, T., Seed, R.B. & Towhata I., Academic Press, New York.
- Panza, G.F., Vaccari, F. & Romanelli F., 2001. Realistic modelling of seismic input in urban areas: a UNESCO- IUGS-IGCP project, *PAGEOPH*, **158**, 2389–2406.
- Pollitz, F., 1999. Regional velocity structure in northern California from inversion of scattered seismic surface waves, *J. geophys. Res.*, **104**, 15 043–15 072.
- Romanelli, F., Bing, Z., Vaccari, F. & Panza G.F., 1996. Analytical computation of reflection and transmission coupling coefficients for Love waves, *Geophys. J. Int.*, **125**, 132–138.
- Sandi, H., Borcia, I.S., Stancu, O. & Stancu M., 2004. Features of sequences of response spectra under successive intermediate depth Vrancea earthquakes, in *Proc. of the 11th International Conference on Soil Dynamics & Earthquake Engineering*, pp. 214–221, eds Doolin, D. et al., Stallion Press, Berkeley.
- Savage, B.K., 2004. Regional Seismic Wavefield Propagation, *PhD thesis*, California Institute of Technology, Pasadena.
- Semblat, J.-F., Duval, A.-M. & Dangla, P., 2000. Numerical analysis of seismic wave amplification in Nice (France) and comparisons with experiments, *Soil Dynam. Earthquake Engrg.*, **19**, 347–362.
- Semblat, J.F., Guéguen, P., Kham, M., Bard, P.-Y. & Duval, A.-M., 2003. Site-city interaction at local and global scales, in *12th European Conference on Earthquake Engineering*, paper no. 807 on CD-ROM, Elsevier, Oxford.
- Semblat, J.F., Parara, E., Kham, M., Bard, P.-Y., Pitilakis, K., Makra, K. & Raptakis, D., 2004. Site effects: basin geometry vs soil layering, in *Proc. 11th International Conference on Soil Dynamics & Earthquake Engineering*, pp. 222–229, eds Doolin, D. et al., Stallion Press, Berkeley.
- Shapiro, N.M., Olsen, K.B. & Singh, S.K., 2000. Wave-guide effects in subduction zones: evidence from three-dimensional modeling, *Geophys. Res. Lett.*, **27**, 433–436.
- Shapiro, N.M., Olsen, K.B. & Singh, S.K., 2002. On the duration of seismic motion incident onto the valley of Mexico for subduction zone earthquakes, *Geophys. J. Int.*, **151**, 501–510.
- Shapiro, N.M., Singh, S.K., Almora, D. & Ayala, M., 2001. Evidence of the dominance of higher-mode surface waves in the lake-bed zone of the valley of Mexico, *Geophys. J. Int.*, **147**, 517–527.
- Shoji, Y., Tani, K. & Kamiyama, M., 2004. A study on the duration and amplitude characteristics of earthquake ground motions, in *Proc. 11th International Conference on Soil Dynamics & Earthquake Engineering*, pp. 157–164, eds Doolin, D. et al., Stallion Press, Berkeley.
- Singh, S.K. & Ordaz, M., 1993. On the origin of long coda observed in the lake-bed strong-motion records of Mexico City, *Bull. seism. Soc. Am.*, **83**, 1298–1306.
- Snieder R., 2000. Surface wave inversions on a regional scale, in *Seismic Modelling of Earth Structure*, pp. 149–181, eds Boschi, E., Ekström, G. & Morelli, A., Compositori, Bologna.
- Trifunac, M.D. & Brady, A.G., 1975. A study on the duration of strong earthquake ground motion, *Bull. seism. Soc. Am.*, **65**, 581–626.
- Trifunac, M.D. & Westermo, B.D., 1976. Dependence of the duration of strong earthquake ground motion on magnitude, epicentral distance, geologic conditions at the recording station and frequency of motion, *Technical Rept. University of Southern California, Dept. Civil Engineering*, CE 76-02.
- Tsogka, C. & Wirgin, A., 2003. Simulation of seismic response in an idealized city, *Soil. Dynam. Earthquake Engrg.*, **23**, 391–402.
- Tuan, H.-S. & Ponamgi, S.R., 1972. Excitation of Love waves in a thin film layer by a line source, *IEEE Trans. Sonics Ultrason.*, **SU-19**, 9–14.
- Van der Hijden, J.H.M.T., 1987. *Propagation of Transient Elastic Waves in Stratified Anisotropic Media*, Springer, New York.
- Whittaker, E.T. & Watson, G.N., 1922. *Modern Analysis*, Chapters 5, 6, Cambridge University Press, Cambridge.
- Wirgin, A., 1988. Love waves in a slab with rough boundaries, *Recent Developments in Surface Acoustic Waves*, pp. 145–155, eds Parker, D.F. & Maugin, G.A., Springer, Berlin.
- Wirgin, A., 2002. Acoustical imaging: classical and emerging methods for applications in macrophysics, in *Scattering*, pp. 95–120, eds Pike, R. & Sabatier, P., Academic, San Diego.
- Wirgin, A. & Kouoh-Bille, L., 1993. Amplification du mouvement du sol au voisinage d'un groupe de montagnes de profil rectangulaire ou triangulaire soumis à une onde sismique SH, in *Génie Parasismique et Aspects Vibratoires dans le Génie Civil*, pp. ES28–ES37, AFPS, Saint-Rémy-lès-Chevreuse.
- Zhang, H.-M., Chen, X.-F. & Chang, S., 2003. An efficient numerical method for computing synthetic seismograms for a layered half-space with sources and receivers at close or same depths, *Pure appl. Geophys.*, **160**, 467–486.